

# Detector simulation challenges for future accelerator experiments

John Apostolakis<sup>1</sup>, Marilena Bandieramonte<sup>2</sup>, Sunanda Banerjee<sup>3</sup>, Nazir Bartosik<sup>4</sup>, Gloria Corti<sup>1</sup>, Gabriele Cosmo<sup>1</sup>, V. Daniel Elvira<sup>5,\*</sup>, Thomas Evans<sup>6</sup>, Andrei Gheata<sup>1</sup>, Simone Pagan Griso<sup>7</sup>, Vladimir Ivantchenko<sup>1</sup>, Christopher Jones<sup>5</sup>, Markus Klute<sup>8</sup>, Charles Leggett<sup>7</sup>, Ben Morgan<sup>9</sup>, Tadej Novak<sup>10</sup>, Kevin Pedro<sup>5</sup>, and Harald Paganetti<sup>11</sup>

<sup>1</sup>European Organization for Nuclear Research (CERN), Organisation Européenne pour la Recherche Nucléaire (CERN), F-01631 Prévessin Cedex, France, CH-1211 Genève 23, Geneva, Switzerland

<sup>2</sup>Department of Physics and Astronomy, University of Pittsburgh, 3941 O'Hara Street., Pittsburgh, PA 15260, United States

<sup>3</sup>Department of Physics, University of Wisconsin, Room 2320 Chamberlin Hall, 1150 University Avenue, Madison, WI 53706-1390, United States

<sup>4</sup>Sezione di Torino, Istituto Nazionale di Fisica Nucleare (INFN), via P. Giuria, 1, 10125 Torino, Italy, Turin

<sup>5</sup>Fermi National Accelerator Laboratory (FNAL), P.O. Box 500, Batavia, IL 60510-0500, United States

<sup>6</sup>Oak Ridge National Laboratory, 1 Bethel Valley Rd., Oak Ridge, TN 37831, United States

<sup>7</sup>Physics Division, Lawrence Berkeley National Laboratory (LBNL), 1 Cyclotron Road, Berkeley, CA 94720-8153, United States

<sup>8</sup>Karlsruhe Institute of Technology (KIT), Kaiserstrasse 12, 76131 Karlsruhe, Germany

<sup>9</sup>Department of Physics, The University of Warwick, Coventry, CV4 7AL, United Kingdom

<sup>10</sup>Deutsches Elektronen-Synchrotron DESY, Notkestr. 85, 22607 Hamburg, Germany

<sup>11</sup>Department of Radiation Oncology, Massachusetts General Hospital and Harvard Medical School, Boston, MA 02114, United States

Correspondence\*:

V.D. Elvira, Fermi National Accelerator Laboratory (FNAL), P.O. Box 500, Batavia, IL 60510-0500, United States  
daniel@fnal.gov

## 2 ABSTRACT

3 Detector simulation is a key component for studies on prospective future high-energy colliders,  
4 the design, optimization, testing and operation of particle physics experiments, and the analysis  
5 of the data collected to perform physics measurements. This review starts from the current state  
6 of the art technology applied to detector simulation in high-energy physics and elaborates on  
7 the evolution of software tools developed to address the challenges posed by future accelerator

8 programs beyond the HL-LHC era, into the 2030-2050 period. New accelerator, detector, and  
9 computing technologies set the stage for an exercise in how detector simulation will serve the  
10 needs of the high-energy physics programs of the mid 21<sup>st</sup> century, and its potential impact on  
11 other research domains.

12 **Keywords:** High Energy Physics, Particle Physics, Radiation, Simulation, Monte Carlo, Software, Computing, High Performance  
13 Computing

## 1 INTRODUCTION

14 Simulation is an essential tool to design, build, and commission the sophisticated accelerator facilities and  
15 particle detectors utilized in experimental high energy physics (HEP). In this context, simulation refers to  
16 a software workflow consisting of a chain of modules that starts with generation of initial particles, for  
17 example, final state particles from a proton-proton collision. A second module simulates the passage of  
18 these particles through the detector geometry and electromagnetic fields, as well as the physics interactions  
19 with its materials. The output contains information about times, positions, and energy deposits of the  
20 particles when they traverse the readout-sensitive components of the detector. In most modern experiments,  
21 this module is based on the Geant4 software toolkit [1, 2, 3] but other packages such as FLUKA [4, 5] and  
22 MARS [6] are also widely used, depending on the application. A third module generates the electronic  
23 signals from the readout components in response to the simulated interactions, outputting this data in the  
24 same format as the real detector system. As such, the datasets generated through simulation may be input  
25 to the same algorithms used to reconstruct physics observables from real data. Simulation is thus not only  
26 vital in designing HEP experiments, it also plays a fundamental role in the interpretation, validation, and  
27 analysis of the large and complex datasets collected by experiments to produce physics results, and its  
28 impact here should not be underestimated [7].

29 With many unanswered questions remaining in particle physics and the end of the Large Hadron Collider  
30 (LHC) program expected in the late 2020s, plans and ideas for the next big facilities of the 2030s-2050s  
31 are gaining momentum. As these facilities intend to explore ever higher energy scales and luminosities,  
32 the scale of simulated data samples needed to design the detectors and their software, and analyze the  
33 physics results will correspondingly grow. Simulation codes will thus face challenges in scaling both their  
34 throughput and accuracy to meet these sample size requirements with finite but ever evolving computational  
35 facilities [8]. The LHC era has already seen a significant evolution of simulation methods from "full"  
36 detailed history-based algorithms to a hybrid of full and "fast" parameterized or machine-learning based  
37 algorithms for the most computationally expensive parts of detectors [9]. A hybrid simulation strategy,  
38 using a combination of full and fast techniques will play a major role for future collider experiments,  
39 but full simulation will still be required to develop and validate the fast algorithms, as well as to support  
40 searches and analyses of rare processes. The goal of this article is to discuss how detector simulation codes  
41 may evolve to meet these challenges in the context of the second and third elements of the above simulation  
42 chain, that is the modeling of the detector, excluding the generation of initial particles (An overview of the  
43 computational challenges here may be found in [8]).

44 Section 2 presents the design parameters of future accelerators and detectors relevant to their simulation  
45 such as colliding particle types, beam parameters, and backgrounds. Challenges in the description and  
46 implementation of complex detector geometries and particle navigation through rapidly varying magnetic  
47 fields and detector elements of different shapes and materials are discussed in Section 3 while the physics  
48 models needed to describe the passage of particles through the detector material at the energy ranges

49 associated with the colliders under consideration will be discussed in Section 4. Beam backgrounds from  
50 particle decay or multiple hard collisions are another important topic of discussion, particularly in the  
51 case of beams with particles that decay or emit synchrotron radiation, and will be discussed in Section 5.  
52 Section 6 focuses on readout modeling in the context of the opportunities and challenges posed by new  
53 detector technology, including novel materials and new generation electronics. Section 7 looks forward  
54 to the computing landscape anticipated in the era of future colliders, and how these technologies could  
55 help improve the physics and computing performance of detector simulation software, and even shape  
56 their future evolution. Section 8 will discuss the evolution of simulation software toolkits, including  
57 how they might adjust to new computing platforms, experiment software frameworks, programming  
58 languages, and the potential success of speculative ideas, as well as the features that would be needed  
59 to satisfy the requirements of future collider physics programs. For decades, HEP has collaborated with  
60 other communities, such as medical and nuclear physics, and space science, on detector simulation codes,  
61 resulting in valuable sharing of research and resources. Section 9 will present examples of application of  
62 detector simulation tools originating in HEP, in particular to the medical field, and how the challenges for  
63 future HEP simulation may overlap.

64 This article is one of the first reviews on the role and potential evolution of detector simulation in far  
65 future HEP collider physics programs. We hope it contributes to highlight its strategic importance both for  
66 HEP and other fields, as well as the need to preserve and grow its priceless community of developers and  
67 experts.

## 2 FUTURE ACCELERATORS AND DETECTORS IN NUMBERS

68 There are several designs for future particle accelerators, each with its strengths and challenges. This  
69 chapter focuses on the accelerator and detector design parameters and issues relevant for software modeling.  
70 In particular, we survey a number of the most mature proposals, including the high luminosity LHC  
71 (HL-LHC), the high energy LHC (HE-LHC), the Large Hadron-electron Collider (LHeC) and its high  
72 luminosity upgrade (HL-LHeC), the Future Circular Collider (FCC) program of ee (electron-positron),  
73 hh (hadron-hadron), and eh (electron-hadron) colliders, the Circular Electron Positron Collider (CEPC),  
74 the Muon Collider, the International Linear Collider (ILC), the Compact Linear Collider (CLIC), and the  
75 Cool Copper Collider (CCC). Table 1 summarizes the parameters of these proposed future accelerators,  
76 including design values for maximal energy, peak luminosity, and integrated luminosity, and references for  
77 each proposal. There are other potential future colliders that are still being designed, including the Super  
78 Proton-Proton Collider (SPPC) [10], an electron-muon collider [11], a muon-proton collider [12], and a  
79 muon-ion collider [13].

80 Modern particle physics accelerators operate with bunched beams and reach peak luminosities higher  
81 than  $1\text{--}2 \times 10^{34} \text{ cm}^{-2} \text{ s}^{-1}$ , exceeding the initial LHC design specification. The luminosity for future  
82 hadron colliders, such as the High Luminosity LHC (HL-LHC), is limited by the maximum number of  
83 simultaneous proton-proton collisions, or pileup, under which the detectors can operate effectively. For  
84 circular lepton colliders at higher energies, the luminosity is limited by the beamstrahlung (deflection-  
85 induced synchrotron radiation), and “top-up” or “top-off” schemes to inject additional particles during  
86 beam circulation are expected to be necessary to extend beam lifetime [14]. For linear machines, design  
87 parameters like the beam size, beam power, beam currents, and repetition rates drive the peak luminosity.

88 Proton-proton collisions offer the greatest energy reach, but they are limited by construction costs and the  
89 availability of high-field magnets. The largest proposed energy comes from the FCC-hh at 100 TeV. Lepton

90 colliders can also push the energy frontier to multiple TeV. The muon collider requires R&D in order to  
91 reduce the transverse and longitudinal beam emittance via cooling and to accelerate to collision energies  
92 all within the muon's  $2.2 \mu\text{s}$  lifetime [15]. However, it offers an exciting path to collision energies up to a  
93 few tens of TeV by suppressing synchrotron radiation relative to electrons. The beam-induced background  
94 (BIB) created by beam muons decaying in flight places new and unique demands on simulation [16].  
95 Wakefield acceleration also offers a possibility for reaching high energies more compactly in the further  
96 future [17].

97 The proposed detector technologies for the next generations of experiments at colliders are growing in  
98 breadth, as indicated by the summary in Table 2. These increases in technological variety are driven by  
99 both physics goals and experimental conditions. In addition, new detectors will be increasing complex and  
100 granular. The interplay between instrumentation and computing is therefore increasingly important, as  
101 detectors become more challenging to simulate. One example is the upcoming High Granularity Calorimeter  
102 (HGCAL) at the Compact Muon Solenoid (CMS) experiment [18]. With roughly six million channels,  
103 it will be the most granular calorimeter built to date. This massively increases the geometry complexity,  
104 leading to a  $\sim 40\text{--}60\%$  increase in the time to simulate the detector [19]; in addition, the increased precision  
105 of the detector is expected to require correspondingly more precise physical models, which may further  
106 double the simulation time in existing software [20]. The incorporation of precision timing information  
107 may also place more demands on the accuracy of the simulation.

108 The HL-LHC is the nearest-future collider surveyed here, and most further-future colliders aim at higher  
109 precision measurements or present even more difficult environments. Therefore, detector complexity  
110 should be expected to continue to increase, in order to facilitate the physics programs and measurements  
111 for these new colliders. More than ever before, increasingly energetic and potentially heavier particles  
112 will interact with the detector materials, and massive increases in accumulated luminosity will enable  
113 physicists to explore the tails of relevant kinematic distributions very precisely. New technologies will  
114 pose their own challenges, such as the muon collider BIB, or new materials whose electromagnetic and  
115 nuclear interactions may not be fully characterized. This motivates the continued development of detector  
116 simulation software, to ensure its computational performance and physical accuracy keep up with the bold  
117 next steps of experimental high energy physics.

### 3 CHALLENGES IN GEOMETRY DESCRIPTION AND NAVIGATION

118 Geometric modeling is a core component of particle transport simulation. It describes both the material  
119 properties of detector components, which condition the particle interactions, and their geometric boundary  
120 limits. Particles are transported through these geometries in small spatial steps, requiring fast and accurate  
121 computation of distances and finding the geometry location after crossing volume boundaries. This task  
122 uses a significant fraction of total simulation time even for the current LHC experiments [8], making  
123 performance a general concern for the evolution of geometry modeling tools. As discussed in section 2,  
124 future detectors will have both higher granularity and interaction rates than the LHC, requiring the geometry  
125 modeling and navigation software to increase the throughput of the above calculations given this increased  
126 complexity. Providing the navigation precision necessary to achieve the required physics accuracy will  
127 likely be challenged by the presence of very thin detectors placed far away from the interaction point.

128 The detector geometry description of a HEP experiment goes through several processing steps between  
129 the initial computer-aided designs (CAD) [21] to the in-memory representation used by the simulation.  
130 These transformations primarily reduce the complexity and level of detail available in the CAD model

131 to increase computing performance without compromising the required physics accuracy. Although the  
132 geometry models at the core of today's HEP detector simulation were designed in the 60's, Geant geometry  
133 implementations [22, 1] have enjoyed continuous success over many generations of CPU architectures  
134 because of a number of features that reduce both the memory footprint and algorithmic complexity. Multiple  
135 volume placements, replication using regular patterns, and hierarchies of non-overlapping 'container'  
136 volumes enable efficient simulation of very complex setups comprising tens of millions of components.  
137 However, creating the model description for such setups is often a long and arduous process, and the  
138 resulting geometry is very difficult to update and optimize.

139 The most popular 3D models used in simulation nowadays are based on primitive solid representations  
140 such as boxes, tubes, or trapezoids, supporting arbitrarily complex Boolean combinations using these  
141 building blocks. Different simulation packages use different constructive solid geometry (CSG) flavours  
142 [23], providing a number of features and model constraints to enhance the descriptive power and  
143 computation efficiency. However, performance can be highly degraded by overuse of some of these  
144 features, such as creating unbalanced hierarchies of volumes or creating overly complex Boolean solids.  
145 Using such inefficient constructs in high occupancy detector regions near the interaction point generally  
146 leads to significant performance degradation.

147 The current geometry implementations have a very limited adaptive capability for optimizing such  
148 inefficient constructs, mainly due to the high complexity of the model building blocks. The geometry  
149 queries can only be decomposed to the granularity of solid primitives, so user-defined constructs cannot  
150 be internally simplified. This calls for investigating surface models as alternatives to today's geometry  
151 representations. Adopting boundary representation (BREP) models [24] composed of first and second-order  
152 algebraic surfaces, would allow decomposing navigation tasks into simple surface queries. An appropriate  
153 choice of the BREP model flavor allowing surface queries to be independent could greatly favor the  
154 highly-parallel workflows of the future.

155 Developing automatic conversion tools from CAD surface-based models to the Geant4 simulation  
156 geometry proved to be too challenging in the past. Supporting surface representations directly in the  
157 simulation geometry would make such conversions possible. This would provide a simpler transition from  
158 the engineering designs to the simulation geometry, having fewer intermediate representations. It would  
159 also make it easier to implement transparent build-time optimizations for inefficient user constructs.

160 Successive upgrades to adapt to new computing paradigms such as object-oriented or parallel design  
161 have not touched the main modelling concepts described above, which served their purpose for decades  
162 of CPU evolution but are quickly becoming a limiting factor for computing hardware with acceleration.  
163 Recent R&D studies [25, 26] have shown that today's state-of-the-art Geant-derived geometry codes such  
164 as VecGeom [27] represent a bottleneck for vectorized or massively parallel workflows. Deep polymorphic  
165 code stacks, low branch predictability, and incoherent memory access are some of the most important  
166 reasons for performance degradation when instruction execution coherence is a hardware constraint. This  
167 is intrinsic to the model being used, combining in the same query algorithms of very different complexity,  
168 called in an unpredictable manner and unfriendly to compiler optimizations. These studies also indicate the  
169 need to simplify the geometry models being used, highly reducing or eliminating unnecessary abstractions.

170 Performance optimization is particularly important for common geometry navigation tasks such as  
171 collision detection of the simulated particle trajectories with the geometry setup, and relocation after  
172 crossing volume boundaries. Navigation helpers are using techniques such as *voxelization* [28] or bounding  
173 volume hierarchies (BVH) [29] to achieve logarithmic complexity in setups having several millions objects.

174 Adopting efficient optimization strategies will be more relevant for the more complex detectors of the  
175 future.

176 The same problem of collision detection is addressed by graphics systems, in particular, ray-tracing (RT)  
177 engines such as NVIDIA OptiX [30] that make use of dedicated hardware acceleration. Adapting HEP  
178 detector simulations to use such engine was implemented in the Opticks library [31], and demonstrated  
179 speedups of more than two orders of magnitude compared to CPU-based Geant4 simulations of optical  
180 photon transport in large liquid-Argon detectors. This required adapting the complete optical photon  
181 simulation workflow to GPUs, but also simplifying and transforming the geometry description to match  
182 OptiX requirements. Generalizing this approach for future HEP detector simulation would require a major  
183 re-engineering effort, in particular for the geometry description. How exactly RT technology evolves  
184 will likely have a big impact on the solutions adopted for detector geometry modeling. As the use of RT  
185 acceleration proliferates in the gaming industry, APIs supported by dedicated languages and libraries  
186 will most probably be made publicly available. Combined with larger on-chip caches, future low-latency  
187 graphics chips may allow externalizing geometry as an accelerated service for simulation. Such service  
188 could become an important booster, but would be conditional to the simplification of the geometry  
189 description and added support for batched multi-track workflows.

190 Evolution in computing technology will most probably present game-changing opportunities to improve  
191 simulation software, as described in Section 7. For example, tensor cores [32] provide a large density  
192 of Flops, although at a cost in precision. Geometry step calculations cannot make use of half-precision  
193 floating point (*FP16*) directly because rounding errors would become too important and affect both physics  
194 precision and transportation over large distances in the detector. Some optimizations may however be  
195 delegated to a *FP16*-based navigation system using ML inference to, for instance, prioritize candidate  
196 searches. Single-precision *FP32*-based geometry distance computation should be given more weight  
197 in the context of the evolution of reduced-precision accelerator-based hardware, because the option to  
198 reduce precision fulfils physics requirements in most cases. Furthermore, it would provide a significant  
199 performance boost due to a smaller number of memory operations for such architectures. Recent studies  
200 report performance gains as large as 40% for certain GPU-based simulation workflows [26], making R&D  
201 in this area a good investment, as long as memory operations remain the dominant bottleneck, even if chips  
202 evolve to provide higher Flops at *FP32* precision or better. The precision reduction option is, however,  
203 not suitable for e.g., micron-thin sensors, where the propagation rounding errors become comparable to  
204 the sensor thickness. Addressing this will require supporting different precision settings depending on the  
205 detector region.

## 4 PHYSICS PROCESSES AND MODELS

206 As mentioned in Sec. 1 Geant4 has emerged as the primary tool to model particle physics detectors. Geant4  
207 offers a comprehensive list of physics models [33] combined with the continuous deployment of new  
208 features and improved functionality, as well as rigorous code verification and physics validation against  
209 experimental data.

### 4.1 Current status

211 During the first two periods of data taking in 2010-2018, the LHC experiments produced, reconstructed,  
212 stored, transferred, and analyzed tens of billions of simulated events. The physics quality of these Geant4-  
213 based Monte Carlo samples produced at unprecedented speed was one of the critical elements enabling  
214 these experiments to deliver physics measurements with greater precision and faster than in previous hadron

215 colliders [7, 34]. Future accelerator programs will, however, require the implementation of additional  
216 physics processes and continuous improvements to the accuracy of existing ones. A quick review of the  
217 current status of physics models in Geant4 will precede a discussion of future needs.

218 Physics in Geant4 are subdivided over several domains, the most relevant for HEP being particle decay,  
219 electromagnetic (EM) interactions, hadronic processes, and optical photon transport. The precision of  
220 the modeling has to be such that it does not become a limiting factor to the potential offered by detector  
221 technology. EM physics interactions of  $e^-/e^+/\gamma$  with the detector material, producing EM showers in  
222 calorimeters, consume a large fraction of the computing resources at the LHC experiments. Reproducing the  
223 response, resolution, and shower shape at a level of a few per mille requires modeling particle showers down  
224 to keV levels, which contain a large number of low-energy secondary particles that need to be produced and  
225 transported through magnetic fields. This level of accuracy is required in order to distinguish EM particles  
226 from hadronic jets, and to efficiently identify overlapping showers. Highly accurate models for energy  
227 deposition in thin calorimeter layers are also essential for reconstruction of charged particles and muons.  
228 Simulation of tracking devices requires accurate modeling of multiple scattering and backscattering at low  
229 and high energy, coupled with very low energy delta electrons. Geant4 delivers on all these requirements  
230 by modeling EM processes for all particle types in the 1 keV to 100 TeV energy range. The accuracy of  
231 Geant4 EM showers is verified by the CMS [35] and ATLAS [36] experiments.

232 Geant4 models physics processes for leptons, long-lived hadrons, and hadronic resonances. Simulation  
233 of particle decay follows recent PDG data. The decay of  $b$ -,  $c$ -quark hadrons and  $\tau$ -leptons is outsourced to  
234 external physics generators via predefined decay mechanisms.

235 Simulation of optical photon production and transport is also provided by Geant4. The main accuracy  
236 limitation arises from the large compute time required to model the large number of photons and the many  
237 reflections that may occur in within the detector. Various methods to speed-up optical photon transport are  
238 available, depending on tolerance to physics approximations.

239 Hadron-nuclear interaction physics models are needed to simulate hadronic jets in calorimeters, hadronic  
240 processes in thin layers of tracking devices, and for simulating shower leakage to the muon chambers.  
241 Geant4 hadronic physics is based on theory models and tuned on thin target data [3]. This approach  
242 guarantees a more reliable predictive power than that offered by parametric models for a wide range of  
243 materials, particle types and energy ranges for which data measurements are not available. Parameter  
244 tuning and model extensions are necessary to describe all particle interactions at all energies [2]. Geant4  
245 has adopted the approach of combining several models that fit the data best in different energy ranges,  
246 since it is unrealistic to expect that one single model would do the job over the full kinematic range of  
247 interest. This is done by providing several sets of predefined "physics lists", which are combinations of  
248 EM and hadronic processes and models. Experiments need to identify the most suitable for their own  
249 physics program by performing the necessary physics validation studies and possibly applying calibration  
250 corrections [36, 37, 35, 38].

## 251 4.2 Future needs

252 The large data volumes to be collected by the HL-LHC experiments will enable experiments to  
253 reduce statistical uncertainties, therefore demanding more accurate simulation to help reduce systematic  
254 uncertainties in background estimation and calibration procedures. The next generation of HEP detectors  
255 to be commissioned at the LHC and designed to operate in future lepton and hadron colliders will have  
256 finer granularity and incorporate novel materials, requiring simulation physics models with improved  
257 accuracy and precision, as well as a broader kinematic coverage. Materials and magnetic fields will also

258 need to be described in more detail to keep systematic uncertainties small. Moreover, new technologies  
259 [39, 40, 41] will allow detectors to sample particle showers with a high time resolution of the order of tens  
260 of picoseconds, which will need to be matched in simulation. Consequently, the simulation community  
261 has launched an ambitious R&D effort to upgrade physics models to improve accuracy and speed, re-  
262 implementing them from the grounds up when necessary (e.g., GeantV [25], Adept [26], Celeritas [42]).  
263 Special attention will be needed to extend accurate physics simulation to the  $O(100)TeV$  domain, including  
264 new processes and models required to support the future collider programs.

265 Achieving an optimal balance between accuracy and software performance will be particularly challenging  
266 in the the case of EM physics, given that the corresponding software module is one of the largest consumers  
267 of compute power [34]. Reviews of EM physics model assumptions, approximations and limitations,  
268 including those for hadrons and ions will be needed to support the HL-LHC and Future Collider (FCC)  
269 programs. The Geant4 description of multiple scattering [43] of charged particles provides predictions in  
270 good agreement with data collected at the LHC. Nevertheless, the higher spatial resolution in new detectors,  
271 [44, 39, 45, 46] may require even higher accuracy to reproduce measured track and vertex resolutions.  
272 Excellent modeling of single-particle scattering and backscattering across Geant4 volume boundaries  
273 for low energy electrons are critical for accurate descriptions of shower shapes in calorimeters, such as  
274 CMS's high granularity hadronic calorimeter. At the very high energies present at the FCC, nuclear size  
275 effects must be taken into account, and elastic scattering models must be extended to include nuclear  
276 form factors in the highest energy range. The description of form factors may affect EM processes at high  
277 energies in such a way that it affects shower shapes and high energy muons. A theoretical description  
278 of the Landau-Pomeranchuk-Migdal (LPM) effect, significant at high energy, is included in the models  
279 describing the bremsstrahlung and pair-production processes in Geant4. For the latter, introducing LPM  
280 leads to differences in cross sections at very high energies that will need to be understood when data  
281 become available. A relativistic pair-production model is essential for simulation accuracy at the FCC. Rare  
282 EM processes like  $\gamma$  conversion to muon and hadron pairs also becomes important at very high energies  
283 and will have to be added. This is also essential to properly model beam background effects in the collision  
284 region of a Higgs Factory. In the cases of the FCC and dark matter search experiments, the description  
285 of pair production will need to be extended to include the emission of a nearby orbital electron (triplet  
286 production) and to take into account nuclear recoil effects. Finally,  $\gamma$  radiative corrections in EM physics  
287 may effects significantly the accuracy of measurements at Higgs factories and will need to be added to  
288 the models. All these rare processes must be added to the simulation to improve the accuracy in the tails  
289 of the physics distributions, where backgrounds become important. These corrections must be included  
290 such that they are invoked only as needed, thus not increasing the computing cost of EM modeling. At the  
291 FCC collision energy, the closeness of tracking devices to the interaction points will also require widening  
292 the range of physics models of short lived particles. This will be particularly important for high-precision  
293 heavy flavor measurements, as non-negligible fractions of beauty and charm hadrons will survive long  
294 enough to intercept beam pipes and the first detector layers. Describing the interaction of such particles with  
295 matter may already be required at the HL-LHC program because of a reduction of the distance between the  
296 trackers and the interaction point [44, 39]. A review of how detector simulation interfaces to dedicated  
297 decay generators during particle transport may be necessary.

298 In hadronic interactions, more than one model is needed to describe QCD physics processes accurately  
299 over the whole energy range. Typically, a hadronic interaction is initiated when a high energy hadron  
300 collides with a nucleon in the nucleus of a given material. This is followed by the propagation of the  
301 secondary particles produced through the nucleus, the subsequent de-excitation of the remnant nucleus  
302 and particle evaporation, until the nucleus reaches the ground state. Different sets of models map naturally



303 to these phases depending on the initial energy of the collision: a parton string model for energy above  
304 few GeV, an intra-nuclear cascade model below that threshold. Pre-compound and de-excitation models  
305 are used to simulate the last steps in the evolution of the interaction. A reliable description of showers in  
306 hadronic calorimeters requires accurate descriptions of all these processes.

307 Geant4 offers two main physics lists to describe hadronic physics in high energy collider experiments.  
308 The main difference between the two consists in the choice of the model describing the initiating quark-  
309 parton phase mentioned above, either a quark-gluon string model, or a Fritiof model [3]. Having more  
310 than one model allows to estimate the systematic uncertainties arising from the approximations they use.  
311 Unfortunately, neither of them is accurate enough to describe the hadronic interactions at multi-TeV  
312 energies occurring at the FCC. New processes will need to be implemented in the hadronic physics  
313 simulation suite to address this higher energy domain, taking inspiration from those available in the EPOS  
314 generator [47], used by the cosmic ray and heavy ion physics communities.

315 Another element essential for the simulation of hadronic physics is precise calculations of interaction  
316 cross-sections. At the highest energies, Geant4 uses a general approach based on the Glauber theory [48],  
317 while at lower energies cross sections are evaluated from tables obtained from the Particle Data Group [49].  
318 This approach profits from the latest thin-target experiment measurements and provide cross-sections for  
319 any type of projectile particle. The precision of cross-section calculations for different types of particles  
320 will need to be improved as more particle types become relevant to particle flow reconstruction in granular  
321 calorimeters.

322 A correct description of particle multiplicity within hadronic showers is also needed to model the  
323 physics performance of highly granular calorimeters (e.g. CMS [50]), and is also essential to simulate  
324 high-precision tracking devices (e.g. LHCb spectrometer). The parameters describing hadronic models  
325 must be tuned to describe all available thin target test beam data, and the models expanded to provide  
326 coverage to as many beam particles and target nuclei as possible. For flavor physics, it is important to take  
327 into account the differences in hadronic cross-sections between particle and anti-particle projectiles.

## 5 BEAM BACKGROUNDS AND PILEUP

328 The main categories of beam backgrounds at  $ee$  colliders are machine and luminosity induced [51]. The  
329 former is due to accelerator operation and includes Synchrotron Radiation (SR) and beam gas interactions.  
330 The latter arises from the interaction of the two beams close to the interaction point of the experiment.

331 The SR that may affect the detector comes from the bending and focusing magnets closest to it. While  
332 detectors will be shielded, a significant fraction of photons may still scatter in the interaction region and be  
333 detected. This is expected to be one of the dominant sources of backgrounds in the FCC- $ee$  detector [52].  
334 Beam gas effects are a result of collisions between the beam and residual hydrogen, oxygen and carbon  
335 gasses in the beam pipe inside the interaction region.

336 The luminosity induced background is generated from the electromagnetic force between the two  
337 approaching bunches, which leads to the production of hard bremsstrahlung photons. These may interact  
338 with the beam and an effect similar to  $e^+e^-$  pair creation can occur, or they scatter with each other which  
339 can result in hadrons, and potentially jets, in the detector. Stray electrons due to scattering between beam  
340 particles in the same bunch can also hit the detector.

341 The main background at  $pp$  colliders are the large number of inelastic proton-proton collisions that  
342 occur simultaneously with the hard-scatter process, collectively known as pileup. This usually results in

343 a number of soft jets coinciding with the collision. The number of interactions per crossing at the future  
344 colliders is expected to exceed one thousand, compared to no more than 200 at the end of the HL-LHC  
345 era. An additional source of luminosity induced background is the cavern background. Neutrons may  
346 propagate through the experimental cavern for a few seconds before they are thermalized, thus producing  
347 a neutron-photon gas. This gas produces a constant background, consisting of low-energy electrons and  
348 protons from spallation.

349 Machine induced backgrounds at  $pp$  colliders are similar to the  $ee$  ones [36]. Besides the beam gas, the  
350 beam halo is a background resulting from interactions between the beam and upstream accelerator elements.  
351 In general, pile-up dominates over the beam gas and beam halo.

352 Muon colliders are special in that the accelerated particles are not stable. The main source of beam  
353 backgrounds are decays of primary muons and the interaction of their decay products with the collider and  
354 detector components [53]. Compared to  $ee$  colliders this represents an additional source of background  
355 resulting in a large number of low momentum particles that may not be stopped by shielding end enter the  
356 interaction region of the detector. Additionally, this type of background needs to be simulated with higher  
357 precision outside of the interaction region.

358 An important consideration is the detector response and readout time compared to the time between  
359 collisions, which is often longer. In-time and out-of-time pile-up should be considered separately. In-time  
360 pileup are additional collisions that coincide with the hard-scatter one, while out-of-time pile-up are  
361 collisions from different bunch crossings than the hard-scatter one, but affect the readout implicitly.

## 362 5.1 Bottlenecks in computational performance

363 The biggest bottleneck in the time it takes to model pileup in a  $pp$  collider is the number of interactions per  
364 bunch crossing. As seen in black circles in Fig. 1 the CPU time requirement has a very steep dependence  
365 on this parameter, which needs to match data-taking conditions. The second issue can be the slow response  
366 time of the detectors, requiring a large number of out-of-time bunch crossings to be simulated. This can  
367 be solved by only simulating the detectors when needed, as not all have the same sensitive time range.  
368 Improvements in detector technologies that will be used in future experiments may make these times small  
369 enough not to cause a significant overhead.

370 Traditionally each in-time or out-of-time interaction is sampled individually and taken into account at the  
371 digitisation step, when detector digital responses are emulated. Experiments pre-sample pile-up events and  
372 reuse them between different samples to reduce computational time [54, 55]. While the pre-sampling itself  
373 still has the same CPU limitations, using those pileup events barely depends on the amount of pileup (red  
374 circles in Fig. 1), but could cause larger stress on storage. Thresholds to analogue signals are applied at  
375 digitization to reduce the amount of saved digits significantly, at the cost of reduced precision when two  
376 digital channels are merged. Thus pre-sampling thresholds need to be tuned for each individual detector,  
377 and computing resources can only be saved by reusing pre-sampled events, where a compromise between  
378 CPU savings and increased storage needs to be made in a way that maintains optimal physics performance.

379 Another option to fully avoid the CPU bottleneck of pileup pre-sampling is to use pileup events from data.  
380 The main bottlenecks here are non-constant detector conditions and alignment. Re-initializing the simulated  
381 geometry adds overheads which may be mitigated by averaging conditions over long periods. However,  
382 this solution will come at the cost of reproducing data less precisely. Furthermore detector readout only  
383 provides digital information above some thresholds which are usually tuned for primary collisions and thus  
384 relatively high. This reduces precision when merging the information with the simulated hard-scatter event.

385 While other types of background are much lower at  $pp$  colliders and their simulation can usually  
386 be skipped, this is not the case for  $ee$  colliders. Some of those backgrounds, e.g. beam gas effects,  
387 synchrotron radiation and intra-beam scattering, happen outside the detector cavern. They are simulated  
388 by the accelerator team as they also affect beam operations. To avoid re-simulating the same type of  
389 background, the simulation can be shared with the experiment as a list of particles that enter the interaction  
390 region [56], though this is still a large number of low-momentum particles to simulate. Experiments thus  
391 also use randomly-triggered collision events for the background estimation, while also being affected by  
392 the threshold effects.

## 393 5.2 Optimal strategy for future colliders

394 During the development stage of the future experiments, detailed simulation of all types of beam  
395 backgrounds is of utmost importance. Simulation provides estimates of the physics impact of backgrounds  
396 and helps to optimize the detector design to minimize them as much as possible [57]. Some backgrounds  
397 can be parametrized or even completely neglected. One such example is that of cavern background neutrons  
398 at hadron colliders. In most cases their contribution is orders of magnitude smaller than that of pileup,  
399 although outer muon chambers would require a detailed description, if high precision is required. As low  
400 momentum neutron simulation is very slow, it can be performed only once and used to derive parametrized  
401 detector responses, which can then be injected at the digitization stage.

402 As discussed earlier in this section, separate simulation of beam backgrounds and pre-digitization saves  
403 computing resources and has a negligible impact on physics performance when reused randomly between  
404 samples. With the increased background rates expected in future colliders, iterative mixing and merging  
405 of background contributions will become an essential technique. Detector readout thresholds must be set  
406 sufficiently low to allow merging of digital signals multiple times with negligible degradation of accuracy.  
407 This would allow iterative pileup pre-sampling, where multiple events with a low number of interactions  
408 could be merged to give an event with a high number of interactions. It would also allow to merge different  
409 types of backgrounds that would be prepared independently. Furthermore, a special set of lower background  
410 thresholds could be setup in the actual detector to enable the use of real data events as background sources.  
411 The latter would yield a reduced performance degradation as compared to current detectors.

412 Most of all the beam background simulation strategy depends on physics accuracy requirements. As  
413 mentioned in Sec. I, current experiments are moving towards a more frequent use of fast simulation  
414 methods, either based on parametrized detector responses or on machine learning technologies. The latter  
415 could be used to choose the precision of the simulation algorithm depending on the event properties, or to  
416 fully generate the background on the fly. Regardless of the choice of the strategy used to simulate large  
417 volumes of physics samples, a detailed modeling as provided by full simulation will always be needed, if  
418 nothing else to derive and tune the faster methods.

## 6 ELECTRONIC SIGNAL MODELING

419 The ambitious physics program at future accelerator-based experiments requires detectors which can  
420 perform very accurate measurements and handle high occupancy at the same time. To achieve these goals,  
421 it is of paramount importance to collect as much information from each individual detector channel as  
422 possible, including the three spatial coordinates, time and energy.

423 For simplicity, this section focuses on two main classes of detectors that pose the most challenges from a  
424 computational point of view: tracking detectors and calorimeters. Those are the ones that usually employ  
425 the largest number of electronic readout channels, thus their behavior needs to be simulated in detail.

426 New generation calorimeters are designed as tracking devices as well as providers of energy deposition  
427 information in the form of the five-dimensional measurement referred to in the first paragraph. These  
428 extended capabilities beyond traditional calorimetric observables present challenges to the simulation  
429 effort, since modeling must achieve accurate descriptions of all these observables simultaneously.  
430 Additionally, calorimeters will often operate in a high-occupancy environment in which sensor and  
431 electronics performance degrade fast as a consequence of radiation damage.

432 The digitization step of simulation takes as input the Geant4-generated analogue signals from the detector.  
433 The first step of the digitization process accumulates this input and groups it for individual read out  
434 elements. This is done in a number of time slots which define the integration time for the detector. Beyond  
435 this step, modeling is highly detector dependent. It is driven by detailed descriptions of readout electronics  
436 including the noise component, cross-talk, and the readout logic which involves the shaping of the signal  
437 and the digitization of the pulse. Finally, a digit is recorded when the signal is above a predefined threshold.

## 438 6.1 Tracking detectors

439 Various types of tracking detectors are currently employed in HEP experiments at colliders [49],  
440 with the most widely used being silicon, gaseous (RPC, MDT, Micromegas, etc), transition-radiation,  
441 and scintillation detectors. Of these, silicon-based detectors are among the most challenging and  
442 computationally expensive to simulate, given the large number of channels and observables involved.

443 Silicon detectors give rise to electron-hole pairs which are collected with a certain efficiency, amplified,  
444 digitized, and recorded. When biased by a voltage difference, the response of the sensor to the passage  
445 of ionizing particles is characterized by its charge collection efficiency ( $CCE$ ) and its leakage current  
446 ( $I_{leak}$ ). As the sensors are operated well above its full depletion voltage, the  $CCE$  is expected to be high.  
447 The current digitization models for silicon detectors are mostly based on a bottom-up approach, where the  
448 overall energy deposit is used to generate multiple electron-hole pairs that are then propagated through a  
449 detailed simulation of the electric field and used to compute the expected signal generated at the electrodes.  
450 Several models are employed for how the overall deposited energy is split. They range from simple models  
451 performing an equal-splitting along the expected trajectory to more complex models [58], each giving  
452 different increasing levels of accuracy at the price of being computationally more expensive.

453 Exposure to radiation induces displacements in the lattice and ionization damage, liberating charge  
454 carriers. These effects contribute to a reduction of the  $CCE$  and an increase in the  $I_{leak}$ . The increase  
455 in instantaneous luminosity projected at the HL-LHC collider challenged experiments to implement  
456 simulation models able to predict the reduced  $CCE$  expected in the presence of radiation damage. A  
457 detailed simulation of the electric field is used with more refined models describing the probability of  
458 charge-trapping and reduced  $CCE$  [59, 60, 61]. Those models tend to be heavy on computing resources,  
459 prompting parametric simulation approaches to be developed as well.

460 Detectors designs for future colliders differ substantially depending on the type of environment they will  
461 have to withstand. Detectors at moderate to high-energy  $e^+e^-$  colliders will see a clean event and moderate  
462 rates of radiation. For such detectors, a detailed simulation strategy is crucial for high precision physics  
463 measurements; however, the demand for large simulated samples makes a hybrid approach including  
464 parametrizations most likely. Silicon-based tracking detectors are also the technology of choice at muon

465 colliders. The radiation environment within this machine poses unique challenges due to the high level of  
466 beam-induced backgrounds (BIBs). Real-time selection of what measurements are most likely to come from  
467 the interaction point rather than from BIBs is likely to rely on detailed shape analyses of the neighboring  
468 pixels that give signals as well as possible correlation across closely-spaced layers [62]. A hybrid approach  
469 will likely be needed, consisting of a detailed simulation of the detector layers where the raw signal  
470 multiplicity is the highest and needs to be reduced, together with a fast simulation approach for the rest of  
471 the tracking detector. For detectors at future hadron colliders, the extreme radiation environment near the  
472 interaction point will make it mandatory to implement radiation damage effects in the simulation. For this,  
473 a parametrized approach would also be the most realistic path to keep computational costs under control.

## 474 6.2 Calorimeters

475 Traditional calorimeters utilize photons generated through the process of scintillation, Cerenkov radiation,  
476 or transition radiation to measure particle energy depositions. Photons are detected by a photo-transducer  
477 where the photons first give rise to electrons and then go through successive steps of amplification  
478 and digitization. Modeling photon transport to the photo-transducers is CPU intensive and traditionally  
479 implemented as a parametrization tuned to predictions obtained from a specialized simulation package [31]  
480 [63]. Nowadays, simulation of optical photons is offloaded to GPUs to mitigate computing costs, taking  
481 advantage of the high levels of parallelism achievable for electromagnetically interacting particles' transport.  
482 The photon transmission coefficient is affected by radiation damage due to formation of color centers in the  
483 medium, thus an assumption is made on the distribution of color centers in the medium. The light output,  
484  $L(d)$ , after receiving a radiation dose  $d$ , is described by an exponential function that depends on the dose:

$$L(d) = L_0 \exp(\mu \cdot d),$$

485 where the parameter  $\mu$  is a property of the material and depends on the dose rate. The radiation damage  
486 parametrizations are typically calibrated from data coming out of a monitoring system. The radiation dose  
487 and the neutron fluence (flux over time) are estimated using an independent simulation of the detector  
488 setup.

489 The next step in the simulation chain for calorimeters is the treatment of the photo transducer, the most  
490 commonly used type being silicon photo-multipliers. These devices also suffer time-dependent effects  
491 related to the radiation exposure: decrease of photo-statistics (fewer photons reaching the device) and  
492 increase of the noise coming from dark currents. The noise increases with the square root of the fluence,  
493 which in turn is proportional to the sensor's area. Signal simulation in silicon photo-multipliers involves:  
494 emulation of photo-statistics using a Poisson distribution, description of the distribution of the photo  
495 electrons according to pulse shape, adjustment of the signal arrival time, as well as the modeling of  
496 the dark current (thermal emission of photo-electrons), the cross-talk among the channels induced in the  
497 neighbors of the fired pixels, the pixel recovery time after being fired, and the saturation effect for large  
498 signals when several photo-electrons fall on the same pixel. An exponential function describes accurately  
499 the re-charge of the pixel as a function of time, while cross-talk can be modeled using a branching Poisson  
500 process. The Borel distribution [64, 65] analytically computes the probability of neighboring cells to fire.

501 Finally, the simulation of the readout electronics includes: the readout gain, adjusted to get an acceptable  
502 signal to noise ratio throughout the life time of the detector); the electronics noise, with contributions  
503 from the leakage current in the detector, the resistors shunting the input to the readout chip, and the  
504 implementation of the so-called common mode-subtraction; and the ADC pulse shape, which decides the

505 fraction of charge leaked to the neighboring bunches. Zero suppression is also modeled, keeping only the  
506 digits which cross a threshold in the time bunch corresponding to sample of interest.

507 In future colliders, simulation of silicon-based calorimeters will face similar challenges than those  
508 described in the previous section for tracking devices. Parametrizations of time consuming photon transport  
509 may be replaced with detailed modeling and processed on computing devices with hardware accelerators.  
510 Radiation damage will be more pronounced in high-background environments such as high-energy hadron  
511 colliders and muon colliders, introducing a time-dependent component all through the signal simulation  
512 chain which will need to be measured from data and modeled in detail.

## 7 COMPUTING

513 Non traditional, heterogeneous architectures, such as GPUs, have recently begun to dominate the design  
514 of new High Performance Computing centers, and are also showing increasing prevalence in data centers  
515 and cloud computing resources. Transitioning HEP software to run on modern system is proving to be a  
516 slow and challenging process, as described in Sec. 7.3. However, in the timescale of future colliders, this  
517 evolution in the computing landscape offers tremendous opportunity to HEP experiments. The predicted  
518 increase in compute power, the capability to offload different tasks to specialized hardware in hybrid  
519 systems, the option to run inference as a service in remote locations in the context of a machine learning  
520 approach, open the field of HEP simulation to a world where simulation data could grow severalfold in  
521 size, while preserving or improving physics models and detector descriptions.

### 7.1 Projection of hardware architecture evolution

523 For example, the U.S. Department of Energy (USDOE) will be standing up three new GPU-accelerated,  
524 exascale platforms in 2023–2024 at the Oak Ridge Leadership Computing Facility (OLCF [66]), Argonne  
525 Leadership Computing Facility (ALCF [67]), and Lawrence Livermore National Laboratory. Additionally,  
526 the National Energy Research Scientific Computing Center (NERSC [68]) is deploying an NVIDIA-  
527 based GPU system for basic scientific research. Figure 2 shows peak performance in Flops for machines  
528 deployed at the OLCF between 2012 and 2023. In addition to the projected  $\sim 55\times$  increase in computing  
529 performance from 2012 to 2022, the percent of peak provided by GPUs has increased from  $\sim 91\%$  to  
530 greater than  $98\%$  over that period. This situation is reflected in computing centers around the world such  
531 as Piz Daint in Switzerland [69], Leonardo in Italy [70], and Karolina in Czechia [71] that heavily use  
532 NVIDIA GPUs, LUMI in Finland [72] that will use AMD GPUs, and MareNostrum 4 in Spain [73] that  
533 uses both NVIDIA and AMD GPUs. Japan’s Fugaku [74], the current leader of the Top 500 supercomputers  
534 list [75], has a novel architecture with very wide registers that behave very much like a GPU. We see  
535 similar heterogeneous computing center designs in smaller institutional clusters, and grid computing sites.  
536 Thus, in order to take advantage of the massive increases in computing capability provided at the HPC  
537 centers, optimizing existing and future simulation codes for GPUs is essential. The other HPCs at the head  
538 of the current Top500 List which do not explicitly use GPUs, such as Fugaku, have hybrid architectures  
539 that have very wide vector processors that offer much the same functionality as traditional GPUs.

540 The primary driver of this evolution is the power requirements driving high-performance computing.  
541 Figure 3 shows power consumption for OLCF machines from 2012 to 2022. Here, we see that for a  $3\times$   
542 increase in total power consumption there is a 17 fold increase in Flops per MW.

543 It is difficult to predict the exact nature of the hardware landscape beyond 5 years or so, but undoubtedly  
544 we will see evolutionary changes of current hardware rather than revolutionary ones - a failed product

545 can now cost billions of dollars due to design and fabrication costs. Core counts will continue to go up,  
546 as transistor feature sizes decrease, with increasing use of multi-chip and 3D stacked solutions needed  
547 to avoid overly large silicon sizes. It is also likely that vendors will devote larger sections of silicon to  
548 specialized functions, such as we see with Tensor and Ray Tracing cores in current GPUs. FPGA and ASIC  
549 vendors are now offering specialized component layouts for domain specific applications, and this level of  
550 customization will likely increase. We are also beginning to see the combination of multiple different types  
551 of cores, such as high and low power CPUs and FPGAs into the same silicon die or chiplet array, leading  
552 to more integrated heterogeneous architectures with faster communication channels between the various  
553 components and much quicker offload speeds.

## 554 7.2 Description of heterogeneous architectures

555 Heterogeneous architectures such as GPUs and FPGAs are fundamentally different from traditional CPU  
556 architectures. CPUs typically possess a small number of complicated cores that excel at branch prediction  
557 and instruction prefetching. They have multiple levels of large, fast caches, and typically have very low  
558 access latencies. GPUs, on the other hand, have a very large number of simple cores (hundreds of thousands  
559 for modern GPUs), that do not handle branch mis-predictions gracefully. GPU cores that are grouped in  
560 a block must operate in lockstep, all processing the same instruction. Branch mis-predictions and thread  
561 divergence will cause a stall, greatly decreasing throughput. GPUs often have much more silicon devoted  
562 to lower and mixed precision operations than they do for double precision calculations, which are heavily  
563 used in High Energy Physics. GPUs are optimized for Single Instruction Multiple Data (SIMD) style of  
564 operations, where sequential threads or cores access sequential memory locations - randomized memory  
565 access causes significant performance degradation. Finally, GPUs have very high access latencies compared  
566 to CPUs - it can take tens of microseconds to offload a kernel from a host to a GPU. The combination of  
567 massive parallelism, memory access patterns, and high latencies of GPUs require a fundamentally different  
568 programming model than that of CPUs.

## 569 7.3 Challenges for software developers

570 All of the GPU manufacturers support programming only with their own software stack. NVIDIA uses  
571 CUDA, AMD promotes HIP, and Intel employs oneAPI. Other heterogeneous architectures such as FPGAs  
572 also use unique programming languages such as Verilog and HLS. The vast majority of current HEP  
573 software is written in C++, and supported by physicists who are usually not professional developers.  
574 Typical HEP workflows encompass millions of lines of code, with hundreds to thousands of kernels, none  
575 of which dominate the computation. In order to target the current diverse range of GPUs and FPGAs,  
576 we would have to rewrite a very large fraction of the HEP software stack in multiple languages. Given  
577 the limited available workforce, and the extremely challenging nature of validating code that executes  
578 differently on multiple architectures, experiments would have to make very difficult choices as to which  
579 hardware they could target, ignoring large amounts of available computing power. Fortunately, we have  
580 seen a number of portability solutions start to emerge recently, such as Kokkos, Raja, Alpaka, and SYCL,  
581 which are able to target more than one hardware backend (see Figure 4). Furthermore, hardware vendors  
582 have seen the benefits of cross platform compatibility, and are working to develop standards which they are  
583 trying to incorporate into the C++ standard. Ideally, a single language or API that could target both CPUs  
584 and all available heterogeneous architectures would be the preferred solution.

585 Currently, mapping computational physics and data codes to GPU architectures requires significant effort  
586 and profiling. Most HEP code bases are not easily vectorizable or parallelizable, and many HEP applications  
587 are characterized by random memory access patterns. They tend to follow sequential paradigms, with many

588 conditional branch points, which make them challenging to adapt to GPUs. Even tasks such as particle  
589 transport, which in high luminosity environments such as the HL-LHC seemingly offer very high levels of  
590 parallelism, are in fact very difficult to run efficiently on GPUs due to rapid thread divergence caused by  
591 non-homogeneous geometrical and magnetic field constraints.

592 One avenue that offers some hope for easier adoption of GPUs is the use of Machine Learning  
593 (ML) techniques to solve physics problems. We are seeing increasing acceptance of ML algorithms  
594 for pattern recognition and feature discrimination tasks in HEP, as well as for more novel tasks such as  
595 generative models for energy depositions in calorimeter simulations. ML backends for all GPU and other  
596 heterogeneous architectures already exist, and are often supported directly by the hardware manufacturers,  
597 which greatly eases the burden for HEP developers.

## 8 SOFTWARE TOOLKITS

598 The evolution of simulation software toolkits will depend greatly on the hardware, whose evolution on the  
599 timescale of 10 years is uncertain as discussed in Section 7. Today's leading toolkit, the Geant4 toolkit [3]  
600 used by most large experiments' detector simulation, and also the particle transport tools FLUKA [5] and  
601 MARS15 [6] used in the assessment of radiation effects, are large, complex, and have evolved over thirty  
602 years of CPU-centric computation.

### 603 8.1 Computing hardware accelerator usage

604 Whether current simulation toolkits can be adapted to profit adequately from a variety of computing  
605 hardware accelerators, principally GPUs, or whether new accelerator-centric codes can be created and then  
606 interfaced into existing toolkits is a key research question. The profitability of the conversion also involves  
607 the effort required for the development of the production level code, and the cost to create GPU-capable  
608 applications. The latter is under active exploration.

609 The research into GPU usage is inspired by efforts in related particle transport applications in HEP and  
610 other fields. As discussed in Secs. 3 and 6, the Opticks project [31] offloads simulation of optical photons  
611 to NVidia GPUs and demonstrates methods to deal with complex specialised geometries on these devices,  
612 specifically ones that have many repetitive structures. MPEXS, a CUDA-based application for medical  
613 physics [76] using Geant4-derived physics models, also demonstrated efficient use of GPU resources for  
614 regular 'voxelised' geometries. However, the general problem of modeling a large range of energies for  
615 particles combined with the full complexities of modern detector geometries has not been tackled yet.  
616 Solving these general problems is the domain of two ongoing R&D efforts, the Celeritas project [42] and  
617 the AdePT prototype [26]. Both are starting by creating CUDA-based proof-of-concept implementations  
618 of electromagnetic physics, and particularly showering, in complex detector geometries on GPUs. Key  
619 goals of the projects include identifying and solving major performance bottlenecks, and providing a  
620 first template for efficiently extracting energy deposits, track passage data, and similar user-defined data.  
621 Initially, both are targeting the simulation of electron, photon, and positron showers in complex geometrical  
622 structures currently described by deep hierarchies with many repetitions of volumes at different levels.  
623 They have identified the need for a geometry modeller adapted for GPUs and accelerators, and sufficiently  
624 capable to handle these complex structures (see Sec. 3). They are in the process of defining and developing  
625 solutions for such a geometry modeller.

626 The limitations of the bandwidth and latency for communication between the CPU and accelerator are an  
627 important constraint in the utilization of GPUs and other accelerators for particle transport simulation, and



628 for the overall application. Minimising the amount of data exchanged, such as input particles and output  
629 hits, between the CPU and accelerator, is an important design constraint for GPU-based particle transport.  
630 The types of detectors for which it is suitable may depend on this. The contention for this resource may  
631 also constrain the overall application which integrates the particle transport and showering with event  
632 generation, generation of signal, and further reconstruction.

633 Existing prototypes such as AdePT and Celeritas strongly focus on keeping computation inside the  
634 accelerator, and moving back to the CPU only the absolute minimum of data and work. When only a  
635 selected region of a geometry is accelerated, a particle which escapes that region must be returned - as must  
636 particle tracks which undergo (rare) interactions not currently simulated in GPU code, e.g. photo-nuclear  
637 interactions. Of course the largest and critical data transferred out of the accelerator are the experiment hit  
638 records (or processed signal sum values) and other user information such as truth information.

639 Early phase exploration of the potential of FPGAs for particle transport is being conducted for medical  
640 physics simulation [77]. Yet the challenges involved appear more daunting, due to the need to compile  
641 a complex tool into hardware. It seems likely that this approach would be investigated only after  
642 implementations are built using 'simpler' building blocks on GPUs. Potentially these will profit from  
643 leveraging implementations created for portable programming frameworks.

644 Based on current trends, except situations where ultimate performance is required for time critical  
645 applications, we expect the established vendor-specific libraries (CUDA, Hip, DPC++) to be slowly  
646 supplanted by the emerging portable programming paradigms (Kokkos, Alpaka, SYCL), and within a few  
647 years a convergence to be established on standard-supported languages and libraries such as C++'s standard  
648 library `std::par` execution policy. With the importance of portability between hardware of different vendors,  
649 it is critical to identify and invest in cross-vendor solutions, and potentially paradigms that can be used to  
650 investigate alternative hardware platforms, as mentioned above for FPGAs.

## 651 8.2 Opportunities for Parallelism

652 We expect applications and future toolkits will need to expose multiple levels of parallelism in order to  
653 manage resources and to coordinate with other computations, such as reconstruction and event generation.  
654 Such levels could entail parallel processing of different events as well as parallel processing of multiple  
655 algorithms or even multiple particles within an event. A detector simulation toolkit cannot assume that it  
656 controls all resources, but must cooperate with other ongoing tasks in the experiment application. At this  
657 point, it is unclear how to accomplish this cooperation efficiently.

658 Seeking to obtain massive parallelism of thousands or tens of thousands of active particles is challenging  
659 to develop in detector simulation. The GeantV project [25] explored the potential of SIMD-CPU based  
660 parallelism by marshalling similar work ('event-based' in the parlance of neutron simulation), e.g. waiting  
661 till many particles entered a particular volume before propagating the particles through that volume. The  
662 project's conclusion was that the speedup potential was modest - between 1.2 and 2.0.

663 It seems clear that the ability to execute many concurrent, independent kernels on recent GPUs is of  
664 crucial interest to HEP, as it avoids the need for very fine grained parallelism at the thread level, which was  
665 the goal of the GeantV project. Given the difficulty of taking advantage of the full available parallelism  
666 of modern GPUs by a single kernel, being able to execute many kernels doing different tasks will be  
667 invaluable.

### 668 8.3 Parametrized Simulation

669 In parallel with the need for a full, detailed simulation capability to meet the physics requirements  
670 of the future colliders, the focus is growing on developing techniques that replace the most CPU-  
671 intensive components of the simulation with faster methods (so called “fast simulation” techniques),  
672 while maintaining an adequate physics accuracy. This category includes optimization/biasing techniques  
673 that aim at tuning parameters concerning simulation constituents such as geometry or physics models and  
674 which are strictly experiment specific, as well as the possibility of parametrizing part of the simulation  
675 (i.e. electromagnetic shower development in calorimeters), by combining different machine learning  
676 techniques. R&D efforts are ongoing in all the major LHC experiments to apply cutting-edge techniques in  
677 generative modelling with deep learning approaches, e.g., GANs, VAEs and normalizing flows, targeting  
678 the description of electromagnetic showers.

679 We expect the bulk production of Monte Carlo simulation data to be performed with a combination of  
680 detailed and parametrized simulation techniques. To this end, enabling the possibility to combine fast and  
681 full simulation tools in a flexible way is of crucial importance. Along these lines, we expect Geant4 to  
682 evolve coherently by providing tools allowing integration of ML techniques with an efficient and smooth  
683 interleaving of different types of simulation.

### 684 8.4 Future of Geant4

685 Due to its versatility, the large number of physics modeling options, and the investment of many  
686 experiments including the LHC experiments, we expect an evolved Geant4 to be a key component of  
687 detector simulation for both the ongoing and the near future experiments well into the 2030s. Over the  
688 next decade, we expect Geant4’s capabilities to evolve to include options for parameterized simulation  
689 using machine learning, and acceleration for specific configurations (geometry, particles and interactions)  
690 on selected hardware, both of which should significantly increase simulation throughput. These enhanced  
691 capabilities will however come with significant constraints, due to the effort required to adapt user code  
692 to the accelerator/heterogeneous computing paradigm. Furthermore, there is a need to demonstrate that  
693 substantial speedup or throughput improvements can be obtained before such an investment in adaptation  
694 of user applications can be undertaken. Full utilization of accelerators may not be required as offloading  
695 some work to accelerators should free up CPU cores to do additional work at the same time thereby  
696 improving throughput. In addition, some HPC sites may require applications to make some use of GPUs in  
697 order to run at the site. Therefore, some minimum GPU utilization by simulation may make it possible  
698 for experiments to run on such HPC resources thereby reducing the total time it takes to do large scale  
699 simulation workflows.

## 9 APPLICATIONS OF HEP TOOLS TO MEDICAL PHYSICS AND OTHER FIELDS

700 After the initial developments of Monte Carlo (MC) methods for the Manhattan project, the tools became  
701 available to the wider research community after declassification in the 1950’s. One of the early adapters of  
702 MC methods were physicists in radiation therapy. Researchers were eager to predict the dose in patients  
703 more accurately as well as designing and simulating detectors for quality assurance and radiation protection.  
704 The simulations were done mainly using in-house developed codes, with some low energy codes modeling  
705 photons up to 20 MeV developed or transferred from basic physics applications [78][33]. Use of MC  
706 tools from the HEP domain mainly started with heavy charged particle therapy, first using protons and  
707 Helium ions and later employing heavier ions such as Carbon ions. Early research here was also done with

708 in-house codes mostly studying scattering in inhomogeneous media. In the early 1990's more and more  
709 high-energy physicists entered the field of medical physics and brought their expertise and codes with them.  
710 Thus started the use of general-purpose MC codes in radiation therapy that were initially developed and  
711 designed for high energy physics applications, such as Geant4 and Fluka. Fruitful collaborations were also  
712 established with the space physics field, with HEP-developed toolkits applied to particle detector design as  
713 well as the similar areas of dosimetry and radiation damage [79].

### 714 9.1 Beam line design and shielding calculations

715 Beam line design and shielding calculations are done prior to installing a treatment device. These  
716 applications of MC are no different to the HEP use case except for the beam energies studied. Beam line  
717 transport would be done by the machine manufacturers and is often based on specialized codes such as,  
718 for instance, Beam Delivery Simulation (BDSIM) [33]. On the other hand, shielding calculations aim at a  
719 conservative estimate with limited required accuracy and would use mostly analytical methods.

720 Shielding calculations are also critical in both manned and unmanned space missions to determine the  
721 radiation environment for humans [80] and instrumentation, as well as detector backgrounds [81].

### 722 9.2 Detector design studies

723 Nuclear and HEP physics hardware developments are frequently finding applications in radiation therapy  
724 and space missions due to similar requirements concerning sensors and real-time data processing. Detectors  
725 are less complex compared to HEP but the components used in simulations are very similar. Differences  
726 are in the particles of interest as well as the energy region of interest. As in HEP, MC simulations are  
727 a powerful tool to optimize detectors and treatment devices [82, 83]. In fact, for radiation therapy or  
728 diagnostic imaging, MC are not only being employed by researchers but also by vendors to optimize their  
729 equipment.

### 730 9.3 Dose calculation

731 Predicting the dose in patients is arguably the most important task in radiation therapy and has therefore  
732 been the most active MC topic [84]. It has similar importance in space physics for predicting dose rates for  
733 astronauts and in materials/electronics [80, 85].

734 Despite its accuracy, MC dose calculation has not found widespread use in treatment planning in medicine.  
735 However, vendors of commercial planning systems have now developed very fast Monte Carlo codes for  
736 treatment planning where millions of histories in thick targets need to be simulated in minutes or seconds  
737 in a very complex geometry, i.e. the patient as imaged with CT [86]. Therefore, these specialized codes  
738 have replaced multi-purpose MC codes that are often less efficient. Multi-purpose codes are however being  
739 used as a gold standard for measurements that are not feasible in humans. In addition, they are often used  
740 to commission treatment planning and delivery workflows. As we are dealing with biological samples such  
741 as patients, scoring functionality often goes beyond about what is typically used in HEP such as scoring  
742 phase spaces on irregular shaped surfaces or dealing with time-dependent geometries.

### 743 9.4 Diagnostic medical imaging

744 MC has long been used in the design of imaging systems such as positron emission tomography (PET) or  
745 computed tomography (CT) [87]. Like in therapy, HEP codes are being applied either directly or tailored  
746 to imaging applications, i.e. for low energy applications [88]. Time of flight as well as optical simulations  
747 are done using MC. In recent years MC is more and more used to also understand interactions in patients.

748 As radiation therapy is pursuing image-guided therapy, imaging devices are also incorporated in treatment  
749 machines resulting in problems that are being studied using MC such as the interaction between magnetic  
750 resonance imaging (MRI) and radiation therapy, either conventional (photon based) or magnetically scanned  
751 proton treatments.

## 752 **9.5 Simulation requirements for non-HEP applications**

### 753 9.5.1 Physics models and data for energy ranges of interest

754 Medical and many space applications typically fall not under high-energy but low-energy physics. HEP  
755 tools might therefore not simulate some effects accurately or their standard settings are not applicable  
756 for low energies and have to be adjusted and potentially even separately validated [89]. Measurements of  
757 fragmentation cross-sections and attenuation curves are needed for MC applications in clinical environments.  
758 Most cross sections and codes are indeed not very accurate for applications outside HEP because materials  
759 and energy regions of interest are very different. In fact, cross sections needed for medical physics  
760 applications go mostly back to experiments done in the 1970's and are no longer of interest to the  
761 basic physics community. For instance, considerable uncertainties in nuclear interaction cross sections  
762 in biological targets are particularly apparent in the simulation of isotope productions [90]. Furthermore,  
763 the interest of high-energy physics is mainly in thin targets whereas medical physics needs accurate  
764 representations of thick target physics to determine energy loss in patients or devices including Coulomb  
765 scattering and nuclear halo. For positively charged particles, the range in tissue materials needs to be  
766 predicted with mm accuracy and 2 accuracy in energy deposition at mm volumes. Novel approaches to  
767 verify treatment rely on detecting secondary gamma radiation outside of the patient requiring accurate  
768 nuclear excitation cross sections in the MeV region.

### 769 9.5.2 Computational efficiency (variance reduction)

770 In the future we may see two types of MC tools in medical physics, i.e. high-efficiency MC algorithms  
771 focusing solely on dose calculation for treatment planning and multi-purpose codes from high energy  
772 physics for research and development. The latter can and will be used more and more to replace difficult or  
773 cumbersome experiments such as detector design studies for dosimetry and imaging. Nevertheless, thick  
774 target simulations are often time consuming and variance reduction techniques have been developed in  
775 medical physics [91] that may also be applicable for high-energy physics applications, as discussed in  
776 Section 8 with cross-fertilization of the two fields.

## 777 **9.6 Future role of MC tools outside of HEP**

778 The main application of high-energy physics tools to other domains will continue to be in detector design,  
779 quality assurance and dose calculation. Furthermore, not only researchers in medical and space physics but  
780 also manufacturers of therapy and detector equipment are employing MC methods to develop new devices.  
781 Whilst these fields may not in general have the extreme requirements on performance and throughput as  
782 the future experiments discussed in Section 2, the improvements necessary here for HEP will benefit other  
783 user communities. By delivering higher accuracy physics with a smaller computational resource for a given  
784 sample size, a commensurate reduction in the costs to research time, money, and environmental impact  
785 will be possible.

786 It is important that collaborations between the many communities utilizing simulation codes are  
787 maintained to ensure sharing of requirements and methodologies to mutual benefit. Medical physics  
788 increasingly overlaps with radiation biology, where research promises a higher clinical impact than pure

789 physics studies, a paradigm shift that became apparent in the last decade. Monte Carlo codes will thus  
790 be applied also in the field of radiation biology and radiation biochemistry [92]. Multiple efforts have  
791 already started, most notably the extensions of Geant4 (Geant4-DNA) and TOPAS (TOPAS-nBio) [93, 94].  
792 These extensions require codes to evolve particularly when it comes to physics in small nanometer volumes  
793 and computational efficiency when using very small step sizes, which may have commonalities with the  
794 geometry developments discussed in Section 3. Figure 5 shows an example of the geometries of typical  
795 size and complexity of molecular structures that are targeted by these simulations. The toolkit/API design  
796 of codes such as Geant4 have been critical in allowing such extensions, as well as allowing development of  
797 a wide range of applications for generic use cases [88, 95, 96, 97]. It is vitally important that HEP MC  
798 codes continue to use this software architecture to allow such innovation and extension. With simulation  
799 geometries, energy regions, materials, particle tracking and scoring that may be very different from HEP  
800 applications, continued exchange of ideas from other user communities will be invaluable in maintaining  
801 and developing HEP simulation codes.

## 10 SUMMARY AND CONCLUSIONS

802 Detector simulation codes such as Geant4, FLUKA, and MARS have played a central part in the  
803 development and operation of the current generation of HEP experiments and in the analysis and  
804 interpretation of their physics results. This critical role will continue as physicists design and plan the next  
805 generation of collider facilities to operate during the mid-21<sup>st</sup>. These experiments, like their predecessors,  
806 will push the boundaries of accelerator and detector technology to explore and improve our knowledge  
807 of fundamental physics. While simulation codes have already been significantly upgraded through the  
808 LHC era to take full advantage of technologies including multi-core CPUs and machine learning, further  
809 evolution will be needed for this software to run on future computing architectures and deliver the large  
810 and accurate data samples demanded by future collider programs.

811 The primary challenges for detector simulation posed by future accelerators and detector designs are  
812 driven by the increased beam luminosities and energies combined with the high granularity (in space and  
813 time) of the proposed detectors. Higher luminosity naturally means that simulations will need to deliver  
814 larger sample sizes to reduce statistical uncertainties in, for example, background estimations, driving an  
815 overall need to increase performance and hence throughput. Corresponding increases in the accuracy and  
816 precision of models for electromagnetic and hadronic physics processes will thus be required to reduce  
817 systematic uncertainties, and to extend their domain of validity to cover higher beam energies and novel  
818 materials. Beam backgrounds will also increase in line with luminosity, and are an especially important  
819 area to model during the design phase of experiments to optimize physics and instrumental backgrounds  
820 therefore improving the precision of physics measurements and extending the reach of new particle searches.  
821 Higher granularity detector systems will challenge current codes for describing their geometries with  
822 the increased number of volumes, as well as propagating particles over large distances while retaining  
823 precision of their intersections with small or thin detector elements. R&D programs are already underway to  
824 explore directions for evolving this critical area of simulation. They are exploring techniques and hardware  
825 used in the computer graphics industry for ray-tracing and Computer-Aided Design (CAD), a particularly  
826 promising direction of research. Both high luminosity and detector granularity impact the final simulation  
827 step of digitization. The increased number of detector readout channels generates a higher computational  
828 load, especially for bottom-up models of signal creation, while the more intense radiation environment will  
829 require time-dependent effects measured from data to be modelled.

830 None of these components of the overall simulation toolkit exist in isolation. For example, the accuracy  
831 of energy depositions in a fine grained tracking calorimeter will be dependent on the interplay between  
832 the physics models and navigation of particles through the geometry elements under the influence of a  
833 magnetic field. Balancing physics accuracy against computing performance will be an important aspect for  
834 experimentalists and simulation code developers to consider. It is clear that employing a hybrid of full and  
835 fast parametrized or ML-based techniques is a realistic strategy for simulating detectors. Fast simulation  
836 may well find application in a broader range of cases than at the present time, either as a full generative  
837 step, or to optimize inputs to, or choice of, full Monte Carlo algorithms. Complete, high throughput, "full"  
838 simulation workflows will nonetheless be required to develop, validate, and tune "fast" methods, as well as  
839 to retrain or optimize them in response to changes in experiment conditions or physics program.

840 While the debate here is driven by the requirements of future HEP collider programs, simulation software  
841 evolves in the context of changes in a broader landscape of developments in hardware and software for High  
842 Performance Computing in academia and industry. The ever rapid pace of technology development limits  
843 predictions of how this may impact HEP over the next five years, let alone the 2040-2050 timescale for  
844 experiments in future collider facilities, but even the current evolutionary trends in GPU, FPGA and other  
845 new architectures offer many exciting opportunities for greater computational power at lower monetary  
846 and environmental cost. Equally, a significant challenge for HEP simulation will be in evolving existing  
847 interfaces and algorithms to effectively utilize this diverse range of emerging architectures. Software  
848 portability tools to assist targeting multiple hardware backends are developing rapidly, and experience  
849 in their use is building within the HEP community. HEP-originated simulation codes have permeated to  
850 other fields requiring modeling of radiation transport, especially in medical, bio-, and space physics. The  
851 collaborations established through this wide range of use cases have lead to many mutually beneficial  
852 developments and impact in both research and industry, and this can be expected, and should be encouraged,  
853 to continue. Though there are differences in energy ranges and detector complexity, increased physics  
854 accuracy and computational efficiency and throughput will be to the benefit of all. Furthermore, new or  
855 novel commonalities may be found, for example in modeling and navigating complex geometries whether  
856 that be a future collider detector or a DNA molecule.

857 Predicting the future for any technological or scientific endeavour can only offer a blurred snapshot of  
858 reality, but it is clear at least that the HEP community will continue to require accurate and computationally  
859 efficient detector simulation codes to develop and utilize its next generation of facilities. Developing  
860 software that meets these requirements presents a major, yet exciting, challenge that will foster collaboration  
861 across fundamental physics, high performance computing and computer science, medical, bio- and space  
862 physics, both in academia and industry. It is this depth and breadth of expertise across domains that will  
863 support and drive innovation in HEP simulation, making this human resource the most important to nurture  
864 and grow to enable the realization of HEP physics programs at future colliders during the second half of  
865 the 21<sup>st</sup> century.

## 11 ADDITIONAL REQUIREMENTS

### CONFLICT OF INTEREST STATEMENT

866 The authors declare that the research was conducted in the absence of any commercial or financial  
867 relationships that could be construed as a potential conflict of interest.

## FUNDING

868 Details of all funding sources should be provided, including grant numbers if applicable. Please ensure to  
869 add all necessary funding information, as after publication this is no longer possible.

870 Ben Morgan is supported by STFC.

871 V. Daniel Elvira, Christopher Jones, and Kevin Pedro are supported by Fermilab, operated by Fermi  
872 Research Alliance, LLC under Contract No. DE-AC02-07CH11359 with the U.S. Department of Energy.

873 Harald Paganetti is in part funded by National Institute of Health: U24 CA215123 (The TOPAS Tool for  
874 Particle Simulation, a Monte Carlo Simulation Tool for Physics, Biology and Clinical Research)

875 Simone Pagan Griso is supported by the U.S. Department of Energy, Office of Science under contract  
876 DE-AC02-05CH11231.

877 Thomas Evans is supported by the Exascale Computing Project (ECP), project number 17-SC-20-SC.  
878 Work for this paper was supported by Oak Ridge National Laboratory (ORNL), which is managed and  
879 operated by UT-Battelle, LLC, for the U.S. Department of Energy (DOE) under Contract No. DEAC05-  
880 00OR22725.

881 Charles Leggett is supported by the DOE HEP Center for Computational Excellence at Lawrence Berkeley  
882 National Laboratory under B&R KA2401045 with the US Department of Energy.

## ACKNOWLEDGMENTS

883 This is a short text to acknowledge the contributions of specific colleagues, institutions, or agencies that  
884 aided the efforts of the authors.

## REFERENCES

- 885 [1] Agostinelli S, Allison J, Amako K, Apostolakis J, Araujo H, Arce P, et al. Geant4—a  
886 simulation toolkit. *Nuclear Instruments and Methods in Physics Research Section A: Accelerators,  
887 Spectrometers, Detectors and Associated Equipment* **506** (2003) 250–303. doi:[https://doi.org/10.  
888 1016/S0168-9002\(03\)01368-8](https://doi.org/10.1016/S0168-9002(03)01368-8).
- 889 [2] Allison J, Amako K, Apostolakis J, Araujo H, Arce Dubois P, Asai M, et al. Geant4 developments  
890 and applications. *IEEE Transactions on Nuclear Science* **53** (2006) 270–278. doi:10.1109/TNS.  
891 2006.869826.
- 892 [3] Allison J, Amako K, Apostolakis J, Arce P, Asai M, Aso T, et al. Recent developments in Geant4.  
893 *Nuclear Instruments and Methods in Physics Research Section A: Accelerators, Spectrometers,  
894 Detectors and Associated Equipment* **835** (2016) 186–225. doi:[https://doi.org/10.1016/j.nima.2016.  
895 06.125](https://doi.org/10.1016/j.nima.2016.06.125).
- 896 [4] Ferrari A, Sala PR, Fassò A, Ranft J. *FLUKA: A multi-particle transport code (program version  
897 2005)*. CERN Yellow Reports: Monographs (Geneva: CERN) (2005). doi:10.5170/CERN-2005-010.
- 898 [5] Böhlen T, Cerutti F, Chin M, Fassò A, Ferrari A, Ortega P, et al. The FLUKA code: Developments  
899 and challenges for high energy and medical applications. *Nuclear Data Sheets* **120** (2014) 211 – 214.  
900 doi:10.1016/j.nds.2014.07.049.
- 901 [6] [Dataset] Mokhov N. MARS15, Version 00 (2016).
- 902 [7] Elvira VD. Impact of detector simulation in particle physics collider experiments. *Physics Reports*  
903 **695** (2017) 1–54. doi:<https://doi.org/10.1016/j.physrep.2017.06.002>.

- 904 [8] The HEP Software Foundation. A roadmap for HEP software and computing R&D for the 2020s.  
905 *Computing and Software for Big Science* **3** (2019) 7. doi:10.1007/s41781-018-0018-8.
- 906 [9] Aad G, et al. AtlFast3: the next generation of fast simulation in ATLAS. *Comput. Softw. Big Sci.* **6**  
907 (2022) 7. doi:10.1007/s41781-021-00079-7.
- 908 [10] Tang J, et al. Concept for a Future Super Proton-Proton Collider (2015).
- 909 [11] Lu M, Levin AM, Li C, Agapitos A, Li Q, Meng F, et al. The physics case for an electron-muon  
910 collider. *Adv. High Energy Phys.* **2021** (2021) 6693618. doi:10.1155/2021/6693618.
- 911 [12] Kaya U, Ketenoglu B, Sultansoy S, Zimmermann F. Luminosity and Physics Considerations on  
912 HL-LHC and HE-LHC based mu-p Colliders (2019).
- 913 [13] Acosta D, Li W. A muon-ion collider at BNL: The future QCD frontier and path to a new energy  
914 frontier of  $\mu+\mu-$  colliders. *Nucl. Instrum. Meth. A* **1027** (2022) 166334. doi:10.1016/j.nima.2022.  
915 166334.
- 916 [14] Talman R. Scaling Behavior of Circular Colliders Dominated by Synchrotron Radiation. *Int. J. Mod.*  
917 *Phys. A* **30** (2015) 1544003. doi:10.1142/S0217751X15440030.
- 918 [15] Delahaye JP, Diemoz M, Long K, Mansoulié B, Pastrone N, Rivkin L, et al. Muon Colliders (2019).
- 919 [16] Bartosik N, et al. Full Detector Simulation with Unprecedented Background Occupancy at a Muon  
920 Collider. *Comput. Softw. Big Sci.* **5** (2021) 21. doi:10.1007/s41781-021-00067-x.
- 921 [17] D'Arcy R, Chappell J, Beinortaite J, Diederichs S, Boyle G, Foster B, et al. Recovery time of a  
922 plasma-wakefield accelerator. *Nature* **603** (2022) 58–62. doi:10.1038/s41586-021-04348-8.
- 923 [18] The Phase-2 Upgrade of the CMS Endcap Calorimeter (2017).
- 924 [19] Pedro K. Current and future performance of the CMS simulation. *EPJ Web Conf.* **214** (2019) 02036.  
925 doi:10.1051/epjconf/201921402036.
- 926 [20] Pedro K. Integration and Performance of New Technologies in the CMS Simulation. *EPJ Web Conf.*  
927 **245** (2020) 02020. doi:10.1051/epjconf/202024502020.
- 928 [21] Hoschek J, Lasser D. *Fundamentals of computer aided geometric design* (AK Peters, Ltd.) (1993).
- 929 [22] Brun R, Bruyant F, Maire M, McPherson AC, Zancarini P. GEANT3 (1987).
- 930 [23] Foley J. *Computer graphics : principles and practice* (Reading, Mass: Addison-Wesley) (1995).
- 931 [24] Stroud I. *Boundary representation modelling techniques* (Springer Science & Business Media)  
932 (2006).
- 933 [25] Amadio G, Ananya A, Apostolakis J, Bandieramonte M, Banerjee S, Bhattacharyya A, et al. GeantV:  
934 Results from the Prototype of Concurrent Vector Particle Transport Simulation in HEP. *Comput.*  
935 *Softw. Big Sci.* **5** (2021) 3. doi:10.1007/s41781-020-00048-6.
- 936 [26] [Dataset] AdePT code repository. <https://github.com/apt-sim/AdePT> (2021).
- 937 [27] Apostolakis J, et al. Towards a high performance geometry library for particle-detector simulations.  
938 *J. of Phys.: Conf. Ser.* **608** (2015) 012023. doi:10.1088/1742-6596/608/1/012023.
- 939 [28] Foley J. *Computer graphics : principles and practice* (Reading, Mass: Addison-Wesley) (1990).
- 940 [29] Larsson T, Akenine-Möller T. A dynamic bounding volume hierarchy for generalized collision  
941 detection. *Computers & Graphics* **30** (2006) 450–459.
- 942 [30] Parker SG, Bigler J, Dietrich A, Friedrich H, Hoberock J, Luebke D, et al. Optix: A general purpose  
943 ray tracing engine. *ACM Trans. Graph.* **29** (2010). doi:10.1145/1778765.1778803.
- 944 [31] Blyth SC. Opticks : GPU optical photon simulation for particle physics using NVIDIA® OptiX™.  
945 *Journal of Physics: Conference Series* **898** (2017) 042001. doi:10.1088/1742-6596/898/4/042001.
- 946 [32] Markidis S, Chien SWD, Laure E, Peng IB, Vetter JS. NVIDIA tensor core programmability,  
947 performance & precision. *CoRR* **abs/1803.04014** (2018).



- 948 [33] Nevay L, Boogert S, Snuverink J, Abramov A, Deacon L, Garcia-Morales H, et al. BDSIM: An  
949 accelerator tracking code with particle–matter interactions. *Computer Physics Communications* **252**  
950 (2020) 107200. doi:https://doi.org/10.1016/j.cpc.2020.107200.
- 951 [34] Apostolakis J, et al. HEP Software Foundation Community White Paper Working Group - Detector  
952 Simulation (2018).
- 953 [35] Sirunyan AM, et al. Measurements of Higgs boson production cross sections and couplings in the  
954 diphoton decay channel at  $\sqrt{s} = 13$  TeV. *JHEP* **07** (2021) 027. doi:10.1007/JHEP07(2021)027.
- 955 [36] Aad G, et al. The ATLAS Simulation Infrastructure. *Eur. Phys. J. C* **70** (2010) 823–874. doi:10.  
956 1140/epjc/s10052-010-1429-9.
- 957 [37] Aad G, et al. Measurements of differential cross-sections in top-quark pair events with a high  
958 transverse momentum top quark and limits on beyond the Standard Model contributions to top-quark  
959 pair production with the ATLAS detector at  $\sqrt{s} = 13$  TeV (2022).
- 960 [38] Sirunyan AM, et al. Performance of missing transverse momentum reconstruction in proton-proton  
961 collisions at  $\sqrt{s} = 13$  TeV using the CMS detector. *JINST* **14** (2019) P07004. doi:10.1088/  
962 1748-0221/14/07/P07004.
- 963 [39] LHCb Collaboration CM. Framework TDR for the LHCb Upgrade II  
964 - Opportunities in flavour physics, and beyond, in the HL-LHC era  
965 . Tech. rep., CERN, Geneva (2021).
- 966 [40] Butler JN, Tabarelli de Fatis T. A MIP Timing Detector for the CMS Phase-2 Upgrade (2019).
- 967 [41] Technical Design Report: A High-Granularity Timing Detector for the ATLAS Phase-II Upgrade.  
968 Tech. rep., CERN, Geneva (2020).
- 969 [42] Johnson S, Tognini S, Canal P, Evans T, Jun S, Lima G, et al. Novel features and GPU performance  
970 analysis for EM particle transport in the Celeritas code. *EPJ Web of Conferences* **251** (2021).  
971 doi:10.1051/epjconf/202125103030.
- 972 [43] Howard A, Ivanchenko V, Novak M, Ribon A. Status of Geant4 simulations of calorimeters. *JINST*  
973 **15** (2020) C05073. doi:10.1088/1748-0221/15/05/C05073.
- 974 [44] Collaboration L. LHCb VELO Upgrade Technical Design Report. Tech. rep. (2013).
- 975 [45] Tumasyan A, et al. The Phase-2 Upgrade of the CMS Tracker (2017).
- 976 [46] Technical Design Report for the ATLAS Inner Tracker Pixel Detector. Tech. rep., CERN, Geneva  
977 (2017).
- 978 [47] Drescher H, Hladik M, Ostapchenko S, Pierog T, Werner K. Parton-based Gribov–Regge theory.  
979 *Physics Reports* **350** (2001) 93–289. doi:https://doi.org/10.1016/S0370-1573(00)00122-8.
- 980 [48] Grichine VM. Integral cross-sections of light nuclei in the Glauber-Gribov representation. *Nucl.*  
981 *Instrum. Meth. B* **427** (2018) 60–62. doi:10.1016/j.nimb.2018.04.044.
- 982 [49] Zyla PA, et al. Review of Particle Physics. *PTEP* **2020** (2020) 083C01. doi:10.1093/ptep/ptaa104.  
983 See the review on *Particle Detectors at Accelerators*.
- 984 [50] The Phase-2 Upgrade of the CMS Endcap Calorimeter (2017).
- 985 [51] Natochii A, Vahsen SE, Nakayama H, Ishibashi T, Terui S. Improved simulation of beam  
986 backgrounds and collimation at SuperKEKB. *Phys. Rev. Accel. Beams* **24** (2021) 081001.  
987 doi:10.1103/PhysRevAccelBeams.24.081001.
- 988 [52] Voutsinas G, Bacchetta N, Boscolo M, Janot P, Kolano A, Perez E, et al. Luminosity- and  
989 Beam- Induced Backgrounds for the FCC-ee Interaction Region Design. *8th International Particle*  
990 *Accelerator Conference* (2017). doi:10.18429/JACoW-IPAC2017-WEPIK004.

- 991 [53] Collamati F, Curatolo C, Lucchesi D, Mereghetti A, Mokhov N, Palmer M, et al. Advanced  
992 assessment of beam-induced background at a muon collider. *JINST* **16** (2021) P11009. doi:10.1088/  
993 1748-0221/16/11/P11009.
- 994 [54] Aad G, et al. Emulating the impact of additional proton-proton interactions in the ATLAS simulation  
995 by pre-sampling sets of inelastic Monte Carlo events. *Comput Softw Big Sci* **6** (2022). doi:10.1007/  
996 s41781-021-00062-2.
- 997 [55] Lange DJ, Hildreth M, Ivantchenko VN, Osborne I. Upgrades for the CMS simulation. *J. Phys. Conf.*  
998 *Ser.* **608** (2015) 012056. doi:10.1088/1742-6596/608/1/012056.
- 999 [56] Altmannshofer W, et al. The Belle II Physics Book. *PTEP* **2019** (2019) 123C01. doi:10.1093/ptep/  
1000 ptz106. [Erratum: PTEP 2020, 029201 (2020)].
- 1001 [57] Dannheim D, Sailer A. Beam-Induced Backgrounds in the CLIC Detectors (2012).
- 1002 [58] Bichsel H. Straggling in Thin Silicon Detectors. *Rev. Mod. Phys.* **60** (1988) 663–699. doi:10.1103/  
1003 RevModPhys.60.663.
- 1004 [59] Aaboud M, et al. Modelling radiation damage to pixel sensors in the ATLAS detector. *JINST* **14**  
1005 (2019) P06012. doi:10.1088/1748-0221/14/06/P06012.
- 1006 [60] Chiochia V, Swartz M, Bortoletto D, Cremaldi L, Cucciarelli S, Dorokhov A, et al. Simulation  
1007 of heavily irradiated silicon pixel sensors and comparison with test beam measurements. *IEEE*  
1008 *Transactions on Nuclear Science* **52** (2005) 1067–1075. doi:10.1109/tns.2005.852748.
- 1009 [61] Swartz M, Fehling D, Giurgiu G, Maksimovic P, Chiochia V. A new technique for the reconstruction,  
1010 validation, and simulation of hits in the CMS pixel detector. *PoS VERTEX2007* (2007) 035.  
1011 doi:10.22323/1.057.0035.
- 1012 [62] Muon Collider Collaboration. Expected Detector Performance at the Muon Collider (????) to appear.
- 1013 [63] Gentit FX. Litrani: a General Purpose Monte-Carlo Program Simulating Light Propagation In  
1014 Isotropic or Anisotropic Media (2001).
- 1015 [64] Vinogradov S. Analytical models of probability distribution and excess noise factor of Solid State  
1016 Photomultiplier signals with crosstalk. *Nucl. Instrum. Meth. A* **695** (2012) 247–251. doi:10.1016/j.  
1017 nima.2011.11.086.
- 1018 [65] Gallego L, Rosado J, Blanco F, Arqueros F. Modeling crosstalk in silicon photomultipliers. *JINST* **8**  
1019 (2013) P05010. doi:10.1088/1748-0221/8/05/P05010.
- 1020 [66] Oak Ridge National Laboratory: Leadership Computing Facility (2022). <https://www.olcf.ornl.gov>.
- 1021 [67] Argonne Leadership Computing Facility (2022). [Online] <https://alcf.anl.gov>.
- 1022 [68] National Energy Research Scientific Computing Center (2022). [Online] <https://www.nersc.gov>.
- 1023 [69] PIZ DAINTE (2022). [Online] <https://www.cscs.ch/computers/piz-daint>.
- 1024 [70] Our supercomputer davinci-1 (2021). [Online] <https://www.leonardo.com/en/innovation-technology/davinci-1-supercomputer>.
- 1025
- 1026 [71] KAROLINA (2020). [Online] <https://www.it4i.cz/en/infrastructure/karolina>.
- 1027 [72] LUMI (2022). [Online] <https://lumi-supercomputer.eu>.
- 1028 [73] Barcelona Supercomputing Center (2022). [Online] <https://www.bsc.es/marenostrum/marenostrum>.
- 1029 [74] Supercomputer Fugaku (2021). [Online] <https://www.fujitsu.com/global/about/innovation/fugaku>.
- 1030 [75] TOP500 LIST—NOVEMBER 2021 (2021). [Online] <https://www.top500.org/lists/top500/list/2021/11/>.
- 1031 [76] Okada S, Murakami K, Incerti S, Amako K, Sasaki T. MPEXS-DNA, a new GPU-based Monte  
1032 Carlo simulator for track structures and radiation chemistry at subcellular scale. *Medical Physics* **46**  
1033 (2019) 1483–1500. doi:https://doi.org/10.1002/mp.13370.
- 1034 [77] Khusainov B, Kerrigan EC, Constantinides GA. Automatic software and computing hardware  
1035 co-design for predictive control. *CoRR* **abs/1710.08802** (2017).

- 1036 [78] Rogers DWO. Fifty years of Monte Carlo simulations for medical physics. *Physics in Medicine and*  
1037 *Biology* **51** (2006) R287–R301. doi:10.1088/0031-9155/51/13/R17.
- 1038 [79] Antin G, Nieminen P, Daly E. Applications of GEANT4 for the ESA space programme (2006), 511  
1039 – 518.
- 1040 [80] Chavy-Macdonald MA, Menicucci A, Santin G, Evans H, Jiggins P, Nieminen P, et al. High-accuracy  
1041 simulations of the ISS radiation environment and applications to interplanetary manned missions.  
1042 *IEEE Transactions on Nuclear Science* **60** (2013) 2427 – 2434. doi:10.1109/TNS.2013.2273375.
- 1043 [81] Eraerds T, Antonelli V, Davis C, Hall D, Hetherington O, Holland A, et al. Enhanced simulations  
1044 on the Athena/Wide Field Imager instrumental background. *Journal of Astronomical Telescopes,*  
1045 *Instruments, and Systems* **7** (2021). doi:10.1117/1.JATIS.7.3.034001.
- 1046 [82] Park H, Paganetti H, Schuemann J, Jia X, Min CH. Monte Carlo methods for device simulations in  
1047 radiation therapy. *Physics in Medicine and Biology* **66** (2021). doi:10.1088/1361-6560/ac1d1f.
- 1048 [83] Baumann KS, Kaupa S, Bach C, Engenhardt-Cabillic R, Zink K. Monte Carlo calculation of  
1049 perturbation correction factors for air-filled ionization chambers in clinical proton beams using  
1050 TOPAS/GEANT. *Zeitschrift fur Medizinische Physik* **31** (2021) 175 – 191. doi:10.1016/j.zemedi.  
1051 2020.08.004.
- 1052 [84] Paganetti H. Range uncertainties in proton therapy and the role of Monte Carlo simulations.  
1053 *International Journal of Radiation Oncology Biology Physics* **86** (2013) 396. doi:10.1016/j.ijrobp.  
1054 2013.02.017.
- 1055 [85] Matthiä D, Hassler D, de Wet W, Ehresmann B, Firan A, Flores-McLaughlin J, et al. The radiation  
1056 environment on the surface of Mars - summary of model calculations and comparison to RAD data.  
1057 *Life Sciences in Space Research* **14** (2017) 18 – 28. doi:10.1016/j.lssr.2017.06.003.
- 1058 [86] Fracchiolla F, Engwall E, Janson M, Tamm F, Lorentini S, Fellin F, et al. Clinical validation of a  
1059 GPU-based Monte Carlo dose engine of a commercial treatment planning system for pencil beam  
1060 scanning proton therapy. *Physica Medica* **88** (2021) 226 – 234. doi:10.1016/j.ejmp.2021.07.012.
- 1061 [87] Costa P, Nersissian D, Umisedo N, Gonzales A, Fernández-Varea J. A comprehensive Monte Carlo  
1062 study of CT dose metrics proposed by the AAPM Reports 111 and 200. *Medical Physics* **49** (2022)  
1063 201 – 218. doi:10.1002/mp.15306.
- 1064 [88] Sarrut D, Bała M, Bardi sM, Bert J, Chauvin M, Chatzipapas K, et al. Advanced Monte Carlo  
1065 simulations of emission tomography imaging systems with GATE. *Physics in Medicine and Biology*  
1066 **66** (2021). doi:10.1088/1361-6560/abf276.
- 1067 [89] Jarlskog C, Paganetti H. Physics settings for using the Geant4 toolkit in proton therapy. *IEEE*  
1068 *Transactions on Nuclear Science* **55** (2008) 1018 – 1025. doi:10.1109/TNS.2008.922816.
- 1069 [90] España S, Zhu X, Daartz J, El Fakhri G, Bortfeld T, Paganetti H. The reliability of proton-nuclear  
1070 interaction cross-section data to predict proton-induced PET images in proton therapy. *Physics in*  
1071 *Medicine and Biology* **56** (2011) 2687 – 2698. doi:10.1088/0031-9155/56/9/003.
- 1072 [91] Ramos-Méndez J, Schuemann J, Incerti S, Paganetti H, Schulte R, Faddegon B. Flagged uniform  
1073 particle splitting for variance reduction in proton and carbon ion track-structure simulations. *Physics*  
1074 *in Medicine and Biology* **62** (2017) 5908–5925. doi:10.1088/1361-6560/aa7831.
- 1075 [92] Plante I. A review of simulation codes and approaches for radiation chemistry. *Physics in Medicine*  
1076 *& Biology* **66** (2021) 03TR02. doi:10.1088/1361-6560/abbd19.
- 1077 [93] Bernal MA, Bordage MC, Brown JMC, Davidková M, Delage E, El Bitar Z, et al. Track structure  
1078 modeling in liquid water: A review of the Geant4-DNA very low energy extension of the Geant4  
1079 Monte Carlo simulation toolkit. *Physica Medica* **31** (2015) 861–874. doi:10.1016/j.ejmp.2015.10.  
1080 087.

- 1081 [94] Schuemann J, McNamara A, Ramos-Méndez J, Perl J, Held K, Paganetti H, et al. TOPAS-nBio:  
1082 An extension to the TOPAS simulation toolkit for cellular and sub-cellular radiobiology. *Radiation*  
1083 *Research* **191** (2019) 125 – 138. doi:10.1667/RR15226.1.
- 1084 [95] Faddegon B, Ramos-Méndez J, Schuemann J, McNamara A, Shin J, Perl J, et al. The TOPAS tool  
1085 for particle simulation, a Monte Carlo simulation tool for physics, biology and clinical research.  
1086 *Physica Medica* **72** (2020) 114–121. doi:10.1118/1.4758060.
- 1087 [96] Santin G, Ivanchenko V, Evans H, Nieminen P, Daly E. GRAS: A general-purpose 3-d modular  
1088 simulation tool for space environment effects analysis. *IEEE Transactions on Nuclear Science* **52**  
1089 (2005) 2294 – 2299. doi:10.1109/TNS.2005.860749.
- 1090 [97] Lei F, Truscott P, Dyer C, Quaghebeur B, Heynderickx D, Nieminen P, et al. MULASSIS: A  
1091 Geant4-based multilayered shielding simulation tool. *IEEE Transactions on Nuclear Science* **49 I**  
1092 (2002) 2788 – 2793. doi:10.1109/TNS.2002.805351.
- 1093 [98] High-Luminosity Large Hadron Collider (HL-LHC): Technical Design Report V. 0.1 **4/2017** (2017).  
1094 doi:10.23731/CYRM-2017-004.
- 1095 [99] Cid Vidal X, et al. Report from Working Group 3: Beyond the Standard Model physics at the HL-LHC  
1096 and HE-LHC. *CERN Yellow Rep. Monogr.* **7** (2019) 585–865. doi:10.23731/CYRM-2019-007.585.
- 1097 [100] Abada A, et al. HE-LHC: The High-Energy Large Hadron Collider: Future Circular Collider  
1098 Conceptual Design Report Volume 4. *Eur. Phys. J. ST* **228** (2019) 1109–1382. doi:10.1140/epjst/  
1099 e2019-900088-6.
- 1100 [101] Bordry F, Benedikt M, Brüning O, Jowett J, Rossi L, Schulte D, et al. Machine Parameters and  
1101 Projected Luminosity Performance of Proposed Future Colliders at CERN (2018).
- 1102 [102] Agostini P, et al. The Large Hadron-Electron Collider at the HL-LHC. *J. Phys. G* **48** (2021) 110501.  
1103 doi:10.1088/1361-6471/abf3ba.
- 1104 [103] Benedikt M, Blondel A, Janot P, Mangano M, Zimmermann F. Future Circular Colliders succeeding  
1105 the LHC. *Nature Phys.* **16** (2020) 402–407. doi:10.1038/s41567-020-0856-2.
- 1106 [104] Abada A, et al. FCC Physics Opportunities: Future Circular Collider Conceptual Design Report  
1107 Volume 1. *Eur. Phys. J. C* **79** (2019) 474. doi:10.1140/epjc/s10052-019-6904-3.
- 1108 [105] Abada A, et al. FCC-ee: The Lepton Collider: Future Circular Collider Conceptual Design Report  
1109 Volume 2. *Eur. Phys. J. ST* **228** (2019) 261–623. doi:10.1140/epjst/e2019-900045-4.
- 1110 [106] Abada A, et al. FCC-hh: The Hadron Collider: Future Circular Collider Conceptual Design Report  
1111 Volume 3. *Eur. Phys. J. ST* **228** (2019) 755–1107. doi:10.1140/epjst/e2019-900087-0.
- 1112 [107] CEPC Conceptual Design Report: Volume 1 - Accelerator (2018).
- 1113 [108] Dong M, et al. CEPC Conceptual Design Report: Volume 2 - Physics & Detector (2018).
- 1114 [109] Schulte D. The International Muon Collider Collaboration. *JACoW IPAC2021* (2021) THPAB017.  
1115 doi:10.18429/JACoW-IPAC2021-THPAB017.
- 1116 [110] Aarons G, et al. ILC Reference Design Report Volume 1 - Executive Summary (2007).
- 1117 [111] Robson A, Burrows PN, Catalan Lasheras N, Linssen L, Petric M, Schulte D, et al. The Compact  
1118 Linear  $e^+e^-$  Collider (CLIC): Accelerator and Detector (2018).
- 1119 [112] The Compact Linear  $e^+e^-$  Collider (CLIC): Physics Potential (2018).
- 1120 [113] Bai M, et al. C<sup>3</sup>: A "Cool" Route to the Higgs Boson and Beyond (2021).

## TABLES

## FIGURES

Collider	Particles	$\sqrt{s}$	Peak lumi. [ $10^{34} \text{ cm}^{-2} \text{ s}^{-1}$ ]	Peak pileup	Total lumi. [ $\text{ab}^{-1}$ ]
HL-LHC [98, 99]	pp	14 TeV	7.5	200	3–4
HE-LHC [100, 99]	pp	27 TeV	16	500	15
LHeC [101, 102]	ep	1.3 TeV	0.5–2.4	0.1	1
HE-LHeC [101, 102]	ep	1.77 TeV	1.5	0.1	2
FCC-ee [103, 104, 105]	ee	88–365 GeV	1.5–230	0	1.5–150
FCC-hh [103, 104, 106]	pp	100 TeV	30	1000	20
FCC-eh [103, 104, 106]	ep	3.5 TeV	1.5	1	2
CEPC [107, 108]	ee	90–240 GeV	32–3	0	2.6–16
Muon Collider [109]	$\mu\mu$	3–14 TeV	1.8–40	*	1–20
ILC [110]	ee	250–500 GeV	2.7–3.6	0	1
CLIC [111, 112]	ee	0.38–3 TeV	1.5–6	0	1–5
CCC [113]	ee	250–550 GeV	1.3–2.4	0	2–4

**Table 1.** The parameters of various future accelerators. \* Muon colliders face beam-induced backgrounds, which have different properties from pileup at ee or pp colliders.

Technology	Tracker	Calorimeter	Muon detector	PID
Solid state	Planar, 3D, MAPS, LGAD, CMOS	Si		LGAD
Gas	TPC, DC	RPC, MPGD	RPC, MPGD, DT, MWPC	TPC, DC, MRPC
Scintillator	SciFi, SiPM	Tiles, fibers, crystals	Panels	
Noble liquid		LAr		
Cherenkov		Quartz fibers		RICH, TOF, TOP, DIRC

**Table 2.** Summary of technologies and applications for future projects.

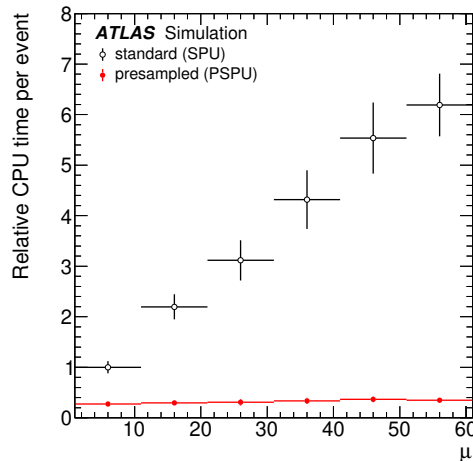


**Figure 1.** Comparison of the average CPU time per event in the standard ATLAS pileup digitization (black open circles) and the pre-sampled pileup digitization (red filled circles) as a function of the number of  $pp$  collisions per bunch crossing ( $\mu$ ). The CPU time is normalized to the time taken for the standard pileup for the lowest  $\mu$  bin. Taken from Ref. [54].

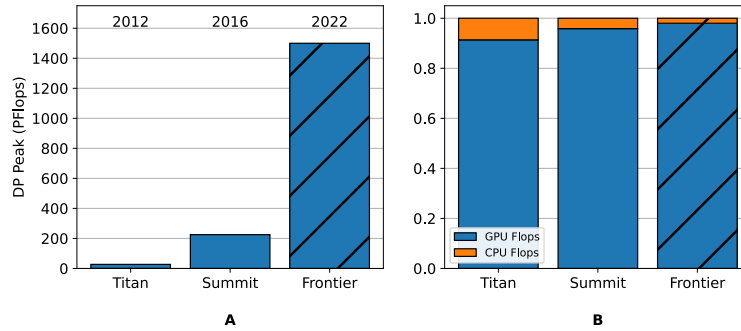


**Figure 2.** Peak performance in Flops (**A**) and fraction of Flops provided by GPU and CPU (**B**) for GPU-accelerated systems deployed at the OLCF. The peak performance for Frontier is projected.

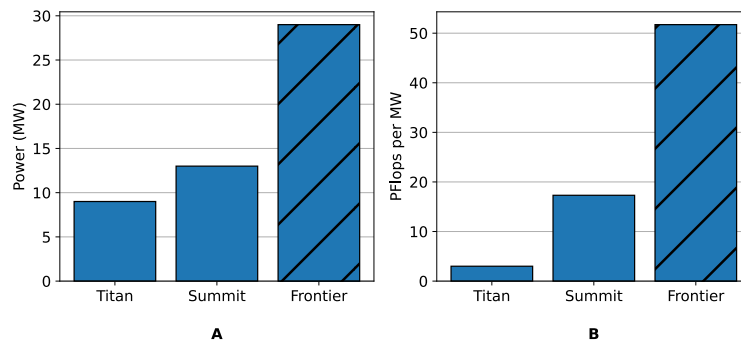


**Figure 3.** Power consumption (**A**) and Flops per MW (**B**) for GPU-accelerated systems deployed at the OLCF. The power requirements for Frontier are projected.

	OpenMP Offload	Kokkos	dpc++ / SYCL	HIP	CUDA	Alpaka	Python	std::par	
NVidia GPU			codeplay and intel/llvm				numba	nvc++	Supported
AMD GPU		feature complete for select GPUs	via hipSYCL and intel/llvm			hip 4.0.1 / clang	numba		Under Development
Intel GPU		native and via OpenMP target offload		HIPLZ: early prototype		prototype	numba-dppy	via oneapi::dpl	3rd Party
CPU single-core									
CPU multi-core								nvc++ g++ & tbb	
FPGA						possibly via SYCL			Not Supported

Figure 4. Portability solutions for heterogeneous architectures.

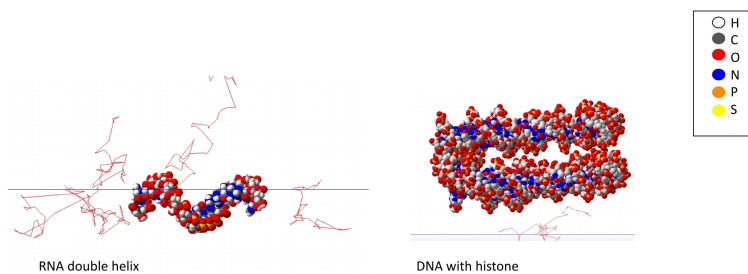


Figure 5. Molecules from the protein data bank read into TOPAS-nBio with a proton track (blue) and secondary electrons (red). Two nucleic acids are shown; an RNA strand and a nucleosome.